The Astrophysical Journal, 773:1 (14pp), 2013 August 10 doi:10.1088/0004-637X/773/1/1

DID THE ANCIENT EGYPTIANS RECORD THE PERIOD OF THE ECLIPSING BINARY ALGOL—THE RAGING ONE?

L. Jetsu[1], S. Porceddu[1], J. Lyytinen[1], P. Kajatkari[1], J. Lehtinen[1], T. Markkanen[1], and J. Toivari-Viitala[2]
[1] Department of Physics, FI-00014 University of Helsinki, P.O. Box 64, Finland; lauri.jetsu@helsinki.fi
[2] Department of World Cultures, FI-00014 University of Helsinki, P.O. Box 59, Finland
Received 2012 November 12; accepted 2013 May 23; published 2013 July 18

ABSTRACT

The eclipses in binary stars give precise information of orbital period changes. Goodricke discovered the 2.867 day period in the eclipses of Algol in the year 1783. The irregular orbital period changes of this longest known eclipsing binary continue to puzzle astronomers. The mass transfer between the two members of this binary should cause a long-term increase of the orbital period, but observations over two centuries have not confirmed this effect. Here, we present evidence indicating that the period of Algol was 2.850 days three millennia ago. For religious reasons, the ancient Egyptians have recorded this period into the Cairo Calendar (CC), which describes the repetitive changes of the Raging one. CC may be the oldest preserved historical document of the discovery of a variable star.

Key words: binaries: eclipsing – history and philosophy of astronomy – methods: statistical – stars: evolution – stars: individual (Algol, Bet Per, HD 19356)

Online-only material: machine-readable table

1. INTRODUCTION

In Algol-type eclipsing binaries (hereafter EBs), one member has evolved away from the main sequence and Roche-lobe overflow has led to mass transfer (hereafter MT) to the other member. MT can increase or decrease the orbital period $P_{\rm orb}$ (Kwee 1958). Many EBs show only positive or negative $P_{\rm orb}$ changes. Alternating period changes (hereafter APCs) seemed to occur only in EBs, where one member displayed magnetic activity (Hall 1989). Activity may explain APC (Applegate 1992), but this phenomenon is still poorly understood (Zavala et al. 2002; Lanza 2006; Liao & Qian 2010).

Montanari discovered Algol in 1669. It was the second variable discovered, 73 yr after the discovery of Mira by Fabricius. Goodricke (1783) determined $P_{\rm orb} = 2\overset{\rm d}{.}867$ of Algol with naked eyes. He received the Copley Medal for this outstanding achievement. The observed (O) eclipses cannot be calculated (C) with a constant $P_{\rm orb}$. These $O-C$ show APC cycles of 1.9, 32, and 180 yr. Algol is actually a triple system. The eclipsing stars in the $2\overset{\rm d}{.}867$ close orbit are Algol A (B8 V) and Algol B (K2 IV). Algol C (F1 IV) in the wide orbit causes the 1.9 yr cycle. Applegate's theory may explain the longer cycles because Algol B has a convective envelope. MT from Algol B to Algol A should cause a long-term $P_{\rm orb}$ increase, but APC may have masked this effect (Biermann & Hall 1973). This problem was discussed when Kiseleva et al. (1998) compared Algol to U Cep, where the parabolic $O-C$ trend has confirmed a $P_{\rm orb}$ increase caused by MT. Evidence for this effect in Algol is lacking after 230 yr of observations. Thus, any $P_{\rm orb}$ information predating 1783 A.D. would be valuable.

Ancient Egyptian Scribes (hereafter AES) wrote Calendars of Lucky and Unlucky Days that assigned good and bad prognoses for the days of the year. These prognoses were based on mythological and astronomical events considered influential for everyday life. The best preserved calendar is the Cairo Calendar (hereafter CC) in papyrus Cairo 86637 dated to 1271–1163 B.C. (Bakir 1966; Demaree & Janssen 1982; Helck et al. 1975–1992). Many CC prognoses had an astronomical origins, because AES acting as "hour watchers" observed bright stars for religious reasons during every clear night (e.g., Leitz 1989, 1994; Krauss 2002, 2012). The traditions of AES in creating and copying tables of various different versions of star clocks spanned thousands of years. We have no exact knowledge about the volume of this activity and admittedly the evidence is scarce, but nevertheless the star clocks required existing astronomical observation practices. The little that we know about the observation practices comes mostly from Late Period (664–332 B.C.) sources such as the inscription on the statue of astronomer Harkhebi and the sighting instrument of Hor, son of Hor-wedja (Clagett 1995). Hardy (2002) argued that CC was a stellar almanac, where known bright stars, like α Car, can be identified. Porceddu et al. (2008, hereafter Paper I) detected the period of the Moon in CC. Indications of a less significant period, $2\overset{\rm d}{.}85$, close to $P_{\rm orb}$ of Algol, were detected, but this connection had to be considered only tentative. Here, we concentrate on statistics, astrophysics, and astronomy. We show that $n \approx 200$ good prognoses would induce $P_{\rm Moon}$ and $P_{\rm Algol}$ in CC, even if the remaining $n \approx 700$ good and bad prognoses had aperiodic origins (Leitz 1994; e.g., diseases, floods, feasts, winds). The connections between Algol and AES are discussed in detail in S. Porceddu et al. (2013, in preparation, hereafter Paper III), where we date CC to 1224 B.C. A shift of $\pm 300^{\rm y}$ would not alter the main results presented here.

2. DATA

The CC prognoses are given in Table 1. The ancient Egyptian year had 365 days. It contained 12 months (M) of 30 days (D). Every month had 3 weeks with 10 days. The year was divided into the flood (Akhet), the winter (Peret), and the harvest (Shemu) seasons. CC gave three prognoses a day, except for the five additional "epagomenal" days of the year. We use the German notation G = "gut" = "good" and S = "schlecht" = "bad" (Leitz 1994). The notation for unreadable prognoses is "–." The Egyptian day began from dawn. Daytime and nighttime were divided into 12 hr. For example, GGS for "I Akhet 25" means that the first two parts of this day were good, but the third part was bad. The logic of this day division procedure has

Table 1
CC Prognoses for One Egyptian Year

Day	Akhet I	Akhet II	Akhet III	Akhet IV	Peret I	Peret II	Peret III	Peret IV	Shemu I	Shemu II	Shemu III	Shemu IV
D	$M=1$	$M=2$	$M=3$	$M=4$	$M=5$	$M=6$	$M=7$	$M=8$	$M=9$	$M=10$	$M=11$	$M=12$
1	GGG	GGG	GGG	GGG	GGG	GGG	GGG	GGG	GGG	GGG	GGG	GGG
2	GGG	GGG	–	GGG	GGG	GGG	GGG	GGG	–	–	GGG	GGG
3	GGS	GGG	GGG	SSS	GGG	–	–	SSS	GGG	GGG	SSS	SSS
4	GGS	SGS	–	GGG	GGG	GGG	GSS	GGG	SSS	SSS	GGG	SSG
5	GGG	SSS	–	GGG	GSS	GGG	GGG	SSS	–	GGG	SSS	GGG
6	SSG	GGG	GGG	SSS	GGG	–	GGG	SSS	GGG	–	–	SSS
7	GGG	SSS	GGG	SSS	SSS	GGG	SSS	GGG	GGG	SSS	SSS	–
8	GGS	GGG	–	GGG	GGG	GGG	GGG	GGG	–	GGG	SSS	GGG
9	GGG	GGG	SSS	GGG	GGG	GGG	GGG	–	GGG	GGG	GGG	GGG
10	GGG	GGG	GGG	GGG	SSS	SSS	SSS	–	–	GGG	SSS	GGG
11	SSS	GGG	GGG	GGG	SSS	GGG	GGG	SSS	–	SSS	SSS	SSS
12	SSS	SSS	–	SSS	–	GGG	GGG	SSS	–	GGG	–	GGG
13	GSS	GGG	SSS	GGG	GGG	SSS	GGG	SSS	–	GGG	–	GGG
14	–	GGG	SSS	GGG	SSS	SGG	–	–	–	GGG	SSS	GGG
15	GSS	GSS	SSS	–	GGG	–	SSS	GGG	–	SSS	GGG	SSS
16	SSS	GGG	GGG	GGG	GGG	–	SSS	GGG	GGG	GGG	SSS	GGG
17	SSS	GGG	–	–	SSS	GGG	SSS	SSS	GGG	SSS	–	GGG
18	GGG	SSS	SSS	SSS	GGG	SSS	GGG	–	GGG	SSS	SSS	SSG
19	GGG	GGG	SSS	SSS	SSS	GSS	–	GGG	GGG	SSS	SSS	GGG
20	SSS	SSS	SSS	SSS	SSS	SSS	SSS	–	SSS	SSS	SSS	–
21	GGG	SSG	GGG	SSG	GGG	–	–	–	SSS	SSG	GGG	GGG
22	SSS	–	–	GGG	GGG	GGG	SSS	SSS	GGG	SSS	SSS	GGG
23	SSS	–	SSS	GGS	GGG	GGG	GGG	–	GGG	GGG	SSS	SSS
24	GGG	SSS	GGG	–	GGG	SSS	SSS	SSS	–	GGG	GGG	GGG
25	GGS	SSS	GGG	–	GGG	GGG	–	SSS	GGG	GGG	GSG	GGG
26	SSS	SSS	GGG	GGG	SSS	–	SSS	–	GGG	SSS	GGG	GSG
27	GGG	SSS	GGG	GGS	GGG	–	SSS	SSS	–	SSS	SSS	SSS
28	GGG	GGG	GGG	SSS	GGG	GGG	GGG	GGG	–	GGG	SSS	GGG
29	SGG	GGG	GGG	SSS	GGG	SSS	GGG	GGG	GGG	GGG	GGG	GGG
30	GGG	GGG	GGG	GGG	GGG	SSS	GGG	GGG	GGG	GGG	GGG	GGG

not been explained anywhere in the known Egyptian texts. The prognosis is usually the same, GGG or SSS, for the whole day. However, 23 days have a heterogeneous prognosis, like GSS. Leitz (1994) used the descriptions of such days to infer how AES divided the day into parts. The first part refers to the morning, the second refers to mid-day, and the third refers to the evening, but may also include the night.

We computed Gregorian days ($N_G = 1 \equiv$January 1) from

$$N_G = \begin{cases} N_E + N_0 - 1, & N_E \leqslant 366 - N_0 \\ N_E + N_0 - 366, & N_E > 366 - N_0, \end{cases} \quad (1)$$

where $N_E = 30(M-1) + D$, and $N_0 = 62$, 187 or 307. Leitz (1994) has suggested $N_0 = 187$. The values $N_0 = 307$ and 62 were obtained by adding 120 and 240 days to $N_0 = 187$. These three N_0 values were tested, because we did not know, where the Gregorian year began in CC. We used $\delta_\odot(N_G) \approx -23.45^\circ \cos[360^\circ(N_G+10)/(365.25)]$. This accuracy was sufficient (see Section 3.6, 11th paragraph). The daytime at Middle Egypt ($\phi = 26^\circ 41'$) was $l_D(N_G) = (24/180^\circ)\{\arccos[-\tan(\phi)\tan(\delta_\odot(N_G))]\}$ hours. Assuming that AES divided $l_D(N_G)$ into three intervals gave

$$\begin{aligned} t_1(N_E) &= (N_E - 1) + (1/6)[l_D(N_G)/24] \\ t_2(N_E) &= (N_E - 1) + (3/6)[l_D(N_G)/24] \\ t_3(N_E) &= (N_E - 1) + (5/6)[l_D(N_G)/24]. \end{aligned} \quad (2)$$

In our other alternative, the daytime was divided into two intervals and the nighttime was the third interval:

$$\begin{aligned} t_1(N_E) &= (N_E - 1) + (1/4)[l_D(N_G)/24] \\ t_2(N_E) &= (N_E - 1) + (3/4)[l_D(N_G)/24] \\ t_3(N_E) &= (N_E - 1) + 1/2 + (1/2)[l_D(N_G)/24]. \end{aligned} \quad (3)$$

These divisions represented the extremes that can be used in placing three epochs within 24 hr. We created 24 different samples of series of time points t_i (hereafter SSTP) from Table 1. The t_i of G and S prognoses were separated. The $D = 1$ and 20 prognoses were always GGG and SSS (Table 1). We removed the t_i of these days from some samples. Table 2 summarizes our SSTP. The t_i values for all prognoses are given in Table 3, which is available in full in the online journal. Columns 1–4 give D, M, N_E, and the prognoses X. Columns 5–10 give t_i calculated for different combinations of Equations (1)–(3).

3. ANALYSIS

We did not analyze the "bivalent data" $y_i = y(t_i) = X(t_i) =$ G or S. We analyzed t_i, which fulfilled $X(t_i) =$ G or S. These "circular data" could be analyzed with numerous nonparametric methods (e.g., Batchelet 1981).

3.1. Rayleigh Test

We analyzed these t_i with a Rayleigh test between $P_{min} = 1\overset{d}{.}5$ and $P_{max} = 90\overset{d}{.}0$. Our P_{min} exceeded the data spacing

Table 2
SSTP = 1, 2, 3, . . ., 23, and 24 Created from Table 1

SSTP	N_0	Div	X	Remove	n	ΔT
1	62	Equation (2)	G	None	564	359.3
2	62	Equation (2)	G	$D = 1$	528	358.3
3	187	Equation (2)	G	None	564	359.4
4	187	Equation (2)	G	$D = 1$	528	358.4
5	307	Equation (2)	G	None	564	359.3
6	307	Equation (2)	G	$D = 1$	528	358.3
7	62	Equation (3)	G	None	564	359.6
8	62	Equation (3)	G	$D = 1$	528	358.6
9	187	Equation (3)	G	None	564	359.6
10	187	Equation (3)	G	$D = 1$	528	358.6
11	307	Equation (3)	G	None	564	359.6
12	307	Equation (3)	G	$D = 1$	528	358.6
13	62	Equation (2)	S	None	351	354.0
14	62	Equation (2)	S	$D = 20$	321	354.0
15	187	Equation (2)	S	None	351	354.0
16	187	Equation (2)	S	$D = 20$	321	354.0
17	307	Equation (2)	S	None	351	354.0
18	307	Equation (2)	S	$D = 20$	321	354.0
19	62	Equation (3)	S	None	351	354.0
20	62	Equation (3)	S	$D = 20$	321	354.0
21	187	Equation (3)	S	None	351	354.0
22	187	Equation (3)	S	$D = 20$	321	354.0
23	307	Equation (3)	S	None	351	354.0
24	307	Equation (3)	S	$D = 20$	321	354.0

Notes. N_0 in Equation (1), day division Div (Equations (2) or (3)), selected prognoses (X), removed prognoses (Remove), sample size (n), and time span ($\Delta T = t_n - t_1$).

(Equations (2) and (3)) and our $P_{\max}$ was $\Delta T/4$. We have applied nonparametric methods to astronomical (Jetsu 1996; Jetsu et al. 1997, 1999, 2000; Lyytinen et al. 2002; Lehtinen et al. 2011, 2012) and geophysical data (Jetsu 1997; Jetsu & Pelt 2000; Lyytinen et al. 2009). The sample size (n) and density ($\Delta T/(nP)$) of CC were better than in any of these previous studies.

The phases are $\phi_i = \mathrm{FRAC}[(t_i - t_0)f]$, where FRAC[$x$] removes the integer part of x, $f = P^{-1}$ is the tested frequency, and t_0 is an arbitrary epoch. Rayleigh *test statistic* is $z(f) = |\mathbf{R}|^2/n$, where $\theta_i = 2\pi\phi_i$, $\mathbf{r}_i = [\cos\theta_i, \sin\theta_i]$ and $\mathbf{R} = \sum_{i=1}^{n} \mathbf{r}_i$. Rayleigh test null hypothesis is

H_0: *"Phases ϕ_i calculated with an arbitrary tested P have a random distribution between 0 and 1."*

If H_0 is true, $\mathbf{r}_i$ point to random directions θ_i and $|\mathbf{R}| \approx 0$. Coinciding θ_i give $|\mathbf{R}| = n$. The probability density function is $f(z) = e^{-z}$, which gives $P(z \leqslant z_0) = F(z_0) = 1 - e^{-z_0}$. If the tested f are between $f_{\min}$ and $f_{\max}$, the number of independent statistical tests is $m = \mathrm{INT}[(f_{\max} - f_{\min})/f_0]$, where INT[$x$] removes the decimal part of x and $f_0 = 1/\Delta T$ (Jetsu & Pelt 1996, 2000). The probability that $z(f)$ exceeds the value z_0 is

$$Q = Q(z_0) = P(z(f) > z_0) = 1 - (1 - e^{-z_0})^m. \quad (4)$$

This Q is the *standard critical level*. We rejected H_0 if

$$Q < \gamma = 0.001, \quad (5)$$

where γ is called the *preassigned significance level.* We used simulations to check if the above standard Q estimates were reliable for the CC data.

Table 4
Number of Different Daily Prognosis Combinations in Table 1

Prognosis	SSTP = 1, 3, . . ., 35			SSTP = 2, 4, . . ., 36		
Combination	Days	G	S	Days	G	S
GGG	177	531	0	165	495	0
GGS	6	12	6	6	12	6
GSG	2	4	2	2	4	2
GSS	6	6	12	6	6	12
SSS	105	0	315	95	0	285
SSG	6	6	12	6	6	12
SGG	2	4	2	2	4	2
SGS	1	1	2	1	1	2
Total	305	564	351	283	528	321
"–"	55	0	0	53	0	0
Total	360	564	351	336	528	321
		⟶ Table 5			⟶ Table 6	

3.2. Simulation of Data Similar to SSTP = 1, 3, . . ., 23

Table 4 summarizes the real data: number of "days" (Columns 2 and 5) having the same "prognosis combination" (Column 1), and number of individual "G" (Columns 3 and 6) or "S" prognoses (Columns 4 and 7). For example, the event $X(t_1)$ = G occurred with the probability of P(Event) = (177+6+2+6)/305 = 191/305 in the *real* data of SSTP = 1, 3, . . ., 23. The complementary event, $X(t_1)$ = S, had P(Event) = (105+6+2+1)/305 = 114/305. We *simulated* aperiodic data, where the prognosis combinations of *real* data occurred with the same probabilities. Table 4 (Columns 2–4) gave the probabilities P(Event) of Table 5. Notations like $X^\star(t_1)$ = G or $X^\star(t_1)$ = S refer to the events that the *simulated* prognosis for the first time point t_1 of an arbitrary day is either G or S. Aperiodic *simulated* data similar to the *real* data in SSTP = 1, 3, . . ., 23 were generated with the following procedure:

Table 3
Time Points t_i for All Prognoses of Table 1

D	M	N_E	X	Div: Equation (2)			Div: Equation (3)		
				$N_0 = 62$ (days)	$N_0 = 187$ (days)	$N_0 = 307$ (days)	$N_0 = 62$ (days)	$N_0 = 187$ (days)	$N_0 = 307$ (days)
1	1	1	G	0.080	0.095	0.076	0.120	0.142	0.114
1	1	1	G	0.239	0.284	0.227	0.359	0.426	0.341
1	1	1	G	0.399	0.473	0.379	0.739	0.784	0.727
2	1	2	G	1.080	1.095	1.076	1.120	1.142	1.113
2	1	2	G	1.240	1.284	1.227	1.360	1.425	1.340

(This table is available in its entirety in a machine-readable form in the online journal. A portion is shown here for guidance regarding its form and content.)

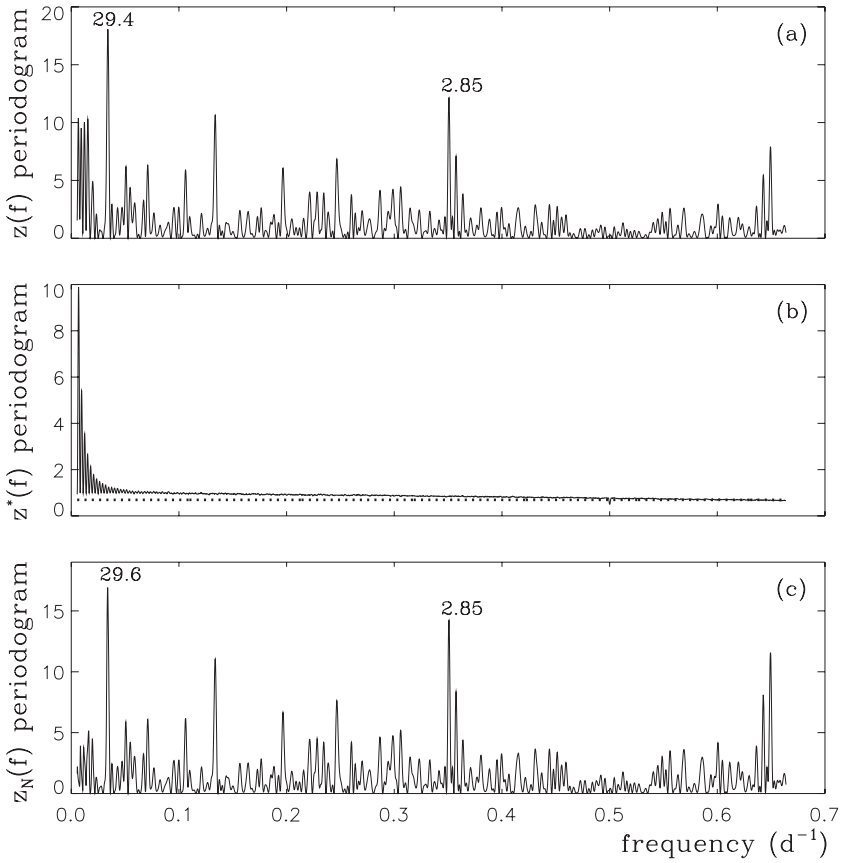

Figure 1. Three periodograms of SSTP = 1. (a) $f(z)$ for *real* data gave $P_1 = 29\overset{d}{.}4$ and $P_2 = 2\overset{d}{.}85$. (b) $z^\star(f)$ (continuous line) for *simulated* data similar to real data and level of $z_0 = 0.693 \equiv Q = 0.5$ (dotted line). (c) $z_N(f)$ for *real* data gave $P_1 = 29\overset{d}{.}6$ and $P_2 = 2\overset{d}{.}85$.

Table 5
Simulation of Aperiodic Data Similar to SSTP = 1, 3,. . . 23

Stage A: Event	*P*(Event)
$X^\star(t_1) = \mathrm{G}$	191/305
$X^\star(t_1) = \mathrm{S}$	114/305
Stage B: Event	***P*(Event)**
$X^\star(t_1) = \mathrm{G} \Rightarrow X^\star(t_2) = \mathrm{G}$	183/191
$X^\star(t_1) = \mathrm{G} \Rightarrow X^\star(t_2) = \mathrm{S}$	8/191
$X^\star(t_1) = \mathrm{S} \Rightarrow X^\star(t_2) = \mathrm{S}$	111/114
$X^\star(t_1) = \mathrm{S} \Rightarrow X^\star(t_2) = \mathrm{G}$	3/114
Stage C: Event	***P*(Event)**
$X^\star(t_1) = \mathrm{G}$ and $X^\star(t_2) = \mathrm{G} \Rightarrow X^\star(t_3) = \mathrm{G}$	177/183
$X^\star(t_1) = \mathrm{G}$ and $X^\star(t_2) = \mathrm{G} \Rightarrow X^\star(t_3) = \mathrm{S}$	6/183
$X^\star(t_1) = \mathrm{G}$ and $X^\star(t_2) = \mathrm{S} \Rightarrow X^\star(t_3) = \mathrm{G}$	2/8
$X^\star(t_1) = \mathrm{G}$ and $X^\star(t_2) = \mathrm{S} \Rightarrow X^\star(t_3) = \mathrm{S}$	6/8
$X^\star(t_1) = \mathrm{S}$ and $X^\star(t_2) = \mathrm{S} \Rightarrow X^\star(t_3) = \mathrm{S}$	105/111
$X^\star(t_1) = \mathrm{S}$ and $X^\star(t_2) = \mathrm{S} \Rightarrow X^\star(t_3) = \mathrm{G}$	6/111
$X^\star(t_1) = \mathrm{S}$ and $X^\star(t_2) = \mathrm{G} \Rightarrow X^\star(t_3) = \mathrm{G}$	2/3
$X^\star(t_1) = \mathrm{S}$ and $X^\star(t_2) = \mathrm{G} \Rightarrow X^\star(t_3) = \mathrm{S}$	1/3

1. We chose the simulated SSTP = 1, 3, . . ., or 23. The t_1, t_2, and t_3 for every N_E were calculated with the N_0 and Div of this SSTP (Table 2). The time points of 55 randomly selected days were removed.
2. The random prognoses for each day were assigned using the probabilities *P*(Event) given in Table 5.

   Stage A. The random prognosis $X^\star(t_1)$ was assigned with the given probabilities *P*(Event).

   Stage B. The result for $X^\star(t_1)$ then determined the probabilities *P*(Event) used in assigning $X^\star(t_2)$.

   Stage C. The results for $X^\star(t_1)$ and $X^\star(t_2)$ then determined *P*(Event) used in assigning $X^\star(t_3)$.
3. We removed t_i with $X^\star(t_i) = \mathrm{S}$ for SSTP = 1, 3, . . ., 11 and t_i with $X^\star(t_i) = \mathrm{G}$ for SSTP = 13, 15, . . ., 23.

We used this procedure to simulate 10,000 samples of aperiodic random t_i similar to every SSTP = 1, 3, . . ., 23. This resembled the bootstrap approach (e.g., Jetsu & Pelt 1996), because we created random samples imitating all the defects of the real data. Our repeated random sampling could also be called the Monte Carlo approach.

The highest $z(f)$ peaks for the *real* data of SSTP = 1 were at $P_1 = 29\overset{d}{.}4$ and $P_2 = 2\overset{d}{.}850$ (Figure 1(a)). They reached $Q = 0.0000034$ and 0.0012. Hence, H_0 should be rejected with P_1, but not with P_2 (Equation (5)).

The *noise periodogram* $z^\star(f)$ for all 10,000 simulated aperiodic data samples similar to SSTP = 1 is shown in Figure 1(b). This $z^\star(f)$ is the *median*, not the *mean*, of $z(f)$ periodograms for all 10,000 simulated data samples at any particular f, because the probability density function of z is not Gaussian. This density function, e^{-z}, predicts that half of the values fulfill $0 \leqslant z \leqslant 0.693$ and the rest fulfill $0.693 < z \leqslant n$. At the higher f, our $z^\star(f)$ approached $z_0 = 0.693 \equiv Q = 0.5$ (Figure 1(b), dotted line). However, $z^\star(f)$ deviated from $z_0 = 0.693$ at lower f, i.e., the standard Q estimates were not reliable. The $z^\star(f)$ periodogram displayed peaks at

$$f = f(\Delta T, k) = [P(\Delta T, k)]^{-1}, \quad (6)$$

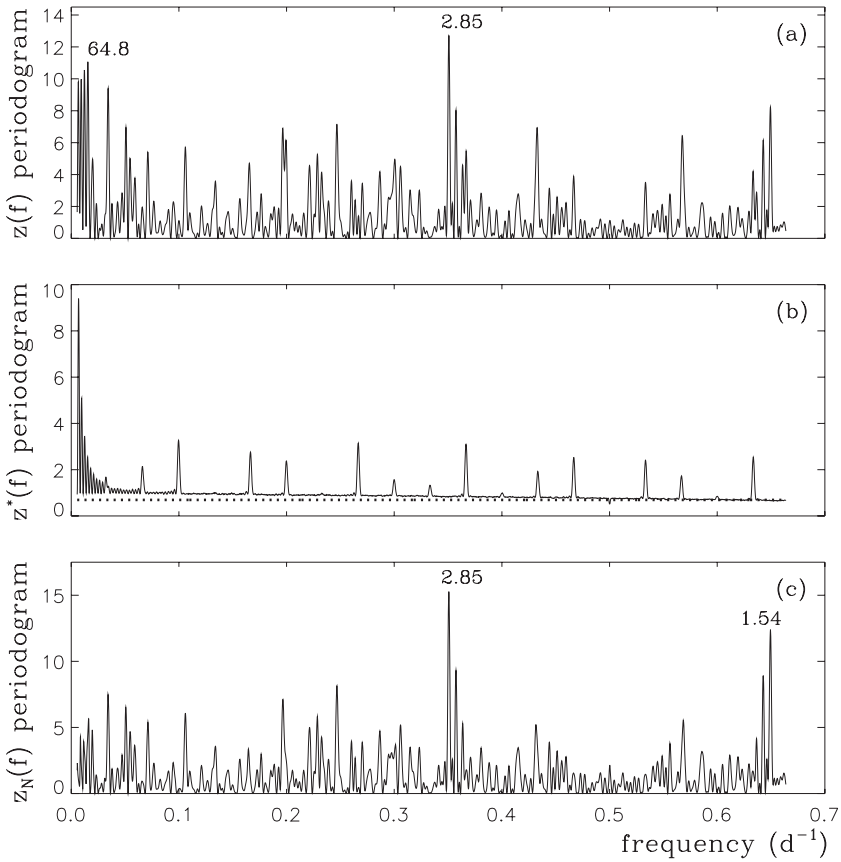

Figure 2. Three periodograms of SSTP = 2.

where $k \geqslant 4$ was an integer and the long periods were $P(\Delta T, k) = \Delta T/(k+1/2)$ (Figure 1(b)). The $n = 564$ simulated t_i were nearly evenly spaced over $\Delta T = 360^{\rm d}$ that contained $k+1/2$ cycles of $P(\Delta T, k)$. The sum of $\mathbf{r}_i$ within the k full cycles was close to zero. The $\mathbf{r}_i$ within the remaining $1/2$ cycle pointed to same side of the unit circle. This caused the $z^\star(f)$ peaks at $f(\Delta T, k)$. These $P(\Delta T, k)$ were unreal periods, which gave us another reason for rejecting the use of the standard Q estimates.

In the power spectrum analysis, the observed power at any tested f is the "signal–power to noise–power ratio" (Scargle 1982). We divided the standard Rayleigh test $z(f)$ periodogram for the real data with the noise periodogram $z^\star(f)$ for similar simulated aperiodic data. This gave us the normalized periodogram

$$z_{\rm N}(f) = z(f)/z^\star(f). \quad (7)$$

To avoid any misunderstanding, we emphasize that the power spectrum method was not applied here. That parametric method relies on a sinusoidal model (Scargle 1982). It can be applied to a time series $y_i = y(t_i)$, but not to a series of time points t_i. Rayleigh test is a nonparametric method. There is no need to fit the data, because there is no model or model parameters.

The highest $z_{\rm N}(f)$ peaks were at $P_1 = 29\overset{\rm d}{.}6$ and $P_2 = 2\overset{\rm d}{.}850$ (Figure 1(c)). Comparison to Figure 1(a) revealed that normalization shifted P_1 from $29\overset{\rm d}{.}4$ to $29\overset{\rm d}{.}6$, but it did not shift P_2. Normalization also eliminated numerous unreal peaks, especially in the lowest f range. We used $z_{\rm N}(f)$ to identify the best periods in SSTP = 1. Their significance also had to be solved from simulations, because the standard Q estimates were unreliable. The peak at $f_1^{-1} = P_1 = 29\overset{\rm d}{.}6$ reached $z_1 = z_{\rm N}(f_1) = 16.68$. We used Table 5 to simulate ten million aperiodic samples similar to the real data of SSTP = 1 and calculated $z_{\rm N}(f)$ for each sample within $[f_1 - f_0/2, f_1 + f_0/2]$. The highest peak satisfied $z_{\rm N}(f) > z_1 = 16.68$ only in 120 of these samples. Hence, the *simulated critical level* for $P_1 = 29\overset{\rm d}{.}6$ was $Q^\star = 0.000012$. For $P_2 = 2\overset{\rm d}{.}850$, the same procedure gave $Q^\star = 0.00014$, which fulfilled the criterion $Q^\star < \gamma = 0.001$. These changes differed, i.e., $Q < Q^\star$ for $P_1 = 29\overset{\rm d}{.}6$ and $Q > Q^\star$ for $P_2 = 2\overset{\rm d}{.}850$. We decided to revise the H_0 rejection criterion to

$$Q^\star < \gamma = 0.001, \quad (8)$$

where Q was substituted with $Q^\star$. The periods $P_3 = 1\overset{\rm d}{.}5401$ ($Q^\star = 0.00091$) and $P_4 = 7\overset{\rm d}{.}48$ ($Q^\star = 0.00091$) also satisfied Equation (8) for SSTP = 1. We will discuss these two unreal periods later.

3.3. Simulation of Data Similar to SSTP = 2, 4, . . ., 24

The sample size decreased after removing the $D = 1$ and 20 prognoses. Columns 5–7 of Table 4 gave the P(Event) of Table 6 used in generating simulated aperiodic data similar to the real data in SSTP = 2, 4, . . ., 24.

1. We chose the simulated SSTP = 2, 4, . . ., or 24. The t_1, t_2, and t_3 for every $N_{\rm E}$ were calculated with the N_0 and Div of this SSTP (Table 2). All time points at $D = 1$ and 20 were first removed. Then the time points of 53 randomly selected days were removed.
2. $X^\star(t_1)$, $X^\star(t_2)$, and $X^\star(t_3)$ values were assigned as in Section 3.2, except that P(event) values were from Table 6.
3. We removed t_i with $X^\star(t_i) =$ S for SSTP = 2, 4, . . ., 12 and t_i with $X^\star(t_i) =$ G for SSTP = 14, 16, . . ., 24.

The highest $f(z)$ peaks for STTP = 2 were at $P_1 = 2\overset{\rm d}{.}850$ and $P_2 = 64\overset{\rm d}{.}8$ (Figure 2(a)). Comparison between Figures 1(b)

Table 6
Simulation of Aperiodic Data Similar to SSTP = 2, 4, . . ., 24

Stage A: Event	P(Event)
$X^\star(t_1) = \mathrm{G}$	179/283
$X^\star(t_1) = \mathrm{S}$	104/283
Stage B: Event	P(Event)
$X^\star(t_1) = \mathrm{G} \Rightarrow X^\star(t_2) = \mathrm{G}$	171/179
$X^\star(t_1) = \mathrm{G} \Rightarrow X^\star(t_2) = \mathrm{S}$	8/179
$X^\star(t_1) = \mathrm{S} \Rightarrow X^\star(t_2) = \mathrm{S}$	101/104
$X^\star(t_1) = \mathrm{S} \Rightarrow X^\star(t_2) = \mathrm{G}$	3/104
Stage C: Event	P(Event)
$X^\star(t_1) = \mathrm{G}$ and $X^\star(t_2) = \mathrm{G} \Rightarrow X^\star(t_3) = \mathrm{G}$	165/171
$X^\star(t_1) = \mathrm{G}$ and $X^\star(t_2) = \mathrm{G} \Rightarrow X^\star(t_3) = \mathrm{S}$	6/171
$X^\star(t_1) = \mathrm{G}$ and $X^\star(t_2) = \mathrm{S} \Rightarrow X^\star(t_3) = \mathrm{G}$	2/8
$X^\star(t_1) = \mathrm{G}$ and $X^\star(t_2) = \mathrm{S} \Rightarrow X^\star(t_3) = \mathrm{S}$	6/8
$X^\star(t_1) = \mathrm{S}$ and $X^\star(t_2) = \mathrm{S} \Rightarrow X^\star(t_3) = \mathrm{S}$	95/101
$X^\star(t_1) = \mathrm{S}$ and $X^\star(t_2) = \mathrm{S} \Rightarrow X^\star(t_3) = \mathrm{G}$	6/101
$X^\star(t_1) = \mathrm{S}$ and $X^\star(t_2) = \mathrm{G} \Rightarrow X^\star(t_3) = \mathrm{G}$	2/3
$X^\star(t_1) = \mathrm{S}$ and $X^\star(t_2) = \mathrm{G} \Rightarrow X^\star(t_3) = \mathrm{S}$	1/3

and 2(b) revealed many new $z^\star(f)$ peaks caused by the removal of t_i at $D = 1$. The standard Q estimates were certainly unreliable. The highest $z_{\mathrm{N}}(f)$ peaks were at $P_1 = 2\overset{\mathrm{d}}{.}850$ ($Q^\star = 0.000094$) and $P_2 = 1\overset{\mathrm{d}}{.}540$ ($Q^\star = 0.00059$) (Figure 2(c)). Normalization did not shift P_1, but it revised P_2 from $64\overset{\mathrm{d}}{.}8$ to $1\overset{\mathrm{d}}{.}540$. This unreal $P_2 = P(\Delta T, k = 5) = 64\overset{\mathrm{d}}{.}8$ was predicted by Equation (6). It was nicely eliminated by normalization.

The most striking *difference* between SSTP = 1 and 2 was that the highly significant $P_1 = 29\overset{\mathrm{d}}{.}6$ vanished. The removal of "GGG" prognoses at $D = 1$ caused this. The most important *similarity* was that the $2\overset{\mathrm{d}}{.}850$ period fulfilled the criterion of Equation (8) in both SSTP = 1 and 2. After removing the $D = 1$ prognoses, the significance of this $2\overset{\mathrm{d}}{.}850$ period increased ($Q^\star = 0.00014 \rightarrow 0.000094$). In conclusion, the removal of $D = 1$ prognoses eliminated the $29\overset{\mathrm{d}}{.}6$ period and the $2\overset{\mathrm{d}}{.}850$ period became the best period. It also became more significant.

The σ_P estimates for all P were determined from $z_{\mathrm{N}}(f)$ with the bootstrap method (Jetsu & Pelt 1996). Table 7 gives the best P for G prognoses. These P satisfied the rejection criterion of Equation (8). All best P for S prognoses (Table 8) failed this criterion of Equation (8).

3.4. Results of the Period Analysis of all G Prognoses

Four periods for G prognoses, $29\overset{\mathrm{d}}{.}6$, $2\overset{\mathrm{d}}{.}85$, $1\overset{\mathrm{d}}{.}54$, and $7\overset{\mathrm{d}}{.}48$, satisfied rejection criterion of Equation (8).

SSTP = 3, 5, 7, 9, and 11 were similar to SSTP = 1 in the sense that the G prognoses at $D = 1$ were not removed. The two best periods for SSTP = 3, 5, 7, 9, and 11 were within the error limits of the two best periods $P_1 = 29\overset{\mathrm{d}}{.}6 \pm 0\overset{\mathrm{d}}{.}2$ and $P_2 = 2\overset{\mathrm{d}}{.}850 \pm 0\overset{\mathrm{d}}{.}002$ for SSTP = 1.

SSTP = 4, 6, 8, 10, and 12 were similar to SSTP = 2, because the $D = 1$ prognoses were removed. The best periods for these five SSTP were within the error limits of the best period $P_1 = 2\overset{\mathrm{d}}{.}850 \pm 0\overset{\mathrm{d}}{.}002$ for SSTP = 2.

We compared the results for the SSTP = 1 and 2 pair in Section 3.3. Comparison of the SSTP = 3 and 4, SSTP = 5 and 6, SSTP = 7 and 8, SSTP = 9 and 10, or SSTP = 11 and 12 pairs showed that removing the G prognoses at $D = 1$ always led to the same result: *the best period* $29\overset{\mathrm{d}}{.}6$ *lost its significance, while* $2\overset{\mathrm{d}}{.}850$ *became the new best period and the significance of this periodicity increased.*

Table 7
Best Periods for the G Prognoses

SSTP	P (days)	$Q^\star$	P (days)	$Q^\star$
1	29.6 ± 0.2	0.000012	2.850 ± 0.002	0.00014
	1.5401 ± 0.0008	0.00091	7.48 ± 0.02	0.00091
2	2.850 ± 0.002	0.000094	1.5400 ± 0.0008	0.00059
3	29.6 ± 0.2	0.000015	2.850 ± 0.002	0.00024
	1.5401 ± 0.0008	0.00057	...	...
4	2.851 ± 0.002	0.00016	1.5401 ± 0.0008	0.00037
5	29.6 ± 0.2	0.000013	2.851 ± 0.002	0.00015
	1.5404 ± 0.0008	0.00081	7.48 ± 0.02	0.00089
6	2.851 ± 0.002	0.000094	1.5401 ± 0.0008	0.00054
7	29.5 ± 0.2	0.000012	2.850 ± 0.002	0.00010
	7.48 ± 0.02	0.00079	...	...
8	2.850 ± 0.002	0.000060	...	...
9	29.6 ± 0.2	0.000012	2.851 ± 0.002	0.00016
	7.48 ± 0.02	0.00090	...	...
10	2.851 ± 0.002	0.000096	...	...
11	29.6 ± 0.2	0.000013	2.851 ± 0.002	0.000076
	7.48 ± 0.02	0.00088	...	...
12	2.851 ± 0.002	0.000051	...	...

Table 8
Best Periods for the S Prognoses

SSTP	P (days)	$Q^\star$	P (days)	$Q^\star$
13	30.3 ± 0.2	0.0021	7.48 ± 0.02	0.0028
14	2.795 ± 0.003	0.0066	1.5570 ± 0.0009	0.0095
15	30.3 ± 0.2	0.0018	7.48 ± 0.02	0.0026
16	2.822 ± 0.002	0.0079	2.795 ± 0.003	0.0084
17	30.3 ± 0.2	0.0020	7.49 ± 0.02	0.0031
18	2.796 ± 0.002	0.0053	1.5487 ± 0.0008	0.011
19	30.2 ± 0.2	0.0018	7.48 ± 0.02	0.0024
20	2.795 ± 0.003	0.0053	2.822 ± 0.002	0.011
21	30.3 ± 0.2	0.0019	7.48 ± 0.02	0.0028
22	2.822 ± 0.002	0.0061	2.795 ± 0.003	0.0068
23	30.3 ± 0.2	0.0021	7.48 ± 0.02	0.0024
24	2.795 ± 0.003	0.0041	2.824 ± 0.002	0.012

The *unreal* $1\overset{\mathrm{d}}{.}54$ period detected in SSTP = 1–6 was predicted by $P'(P_0, k_1, k_2) = [P^{-1} + (k_1/(k_2 P_0)]^{-1}$, where $P = 2\overset{\mathrm{d}}{.}85$ is the real period, $P_0 = 1\overset{\mathrm{d}}{.}0$ is the window period, $k_1 = -1$ and $k_2 = 1$ (Tanner 1948). This unreal period was not detected in SSTP = 7–12, because the daily t_i were evenly distributed over 24 hr with Equation (3) and therefore induced no $P_0 = 1\overset{\mathrm{d}}{.}0$ window period.

We detected the *unreal* $7\overset{\mathrm{d}}{.}48$ period in SSTP = 1, 5, 7, 9, and 11, but it vanished in SSTP = 2, 6, 8, 10, and 12, because it was nearly equal to $\delta t/4 = 7\overset{\mathrm{d}}{.}50$, where $\delta t = 30^{\mathrm{d}}$ was the distance between the removed $D = 1$ prognoses.

Normalization shifted the best period from $29\overset{\mathrm{d}}{.}4$ to $29\overset{\mathrm{d}}{.}6$ in SSTP = 1 (Figures 1(a) and (c)). It caused similar shifts in SSTP = 3, 5, 7, 9, and 11. These shifts were always toward the mean of the synodic month, $P_{\mathrm{syn}} = 29\overset{\mathrm{d}}{.}53$, which would have

been the most practical value for prediction purposes of AES. The synodic month is not constant, but varies between $29\overset{d}{.}3$ and $29\overset{d}{.}8$ in a year (Stephenson & Baolin 1991). Our $P_{\rm Moon}$ differed from $29\overset{d}{.}53$ only by $+0\overset{d}{.}07$ (SSTP = 1, 3, 5, 9, and 11) and $-0\overset{d}{.}03$ (SSTP = 7). We solved the precision σ_P that AES could have reached from n observations of $P_i = P_{\rm syn} + (A_{\rm Moon}/2)\sin(2\pi x_i)$, where $A_{\rm Moon} = 0\overset{d}{.}5$, $x_i = i/n$ and $i = 1, \ldots, n$. It was $\sigma_P^2 = [(A_{\rm Moon}/2)^2/n] \sum_{i=1}^{n} [\sin(iu)]^2$, where $u = 2\pi/n$. Then $\sum_{i=1}^{n} [\sin(iu)]^2 = n/2 - [\cos(n+1)u \sin(nu)]/[2\sin u]$ (Gradshteyn & Ryzhik 1994) gave $\sigma_P = 2^{-3/2} A_{\rm Moon} = 0\overset{d}{.}18$. This agreed with our $\sigma_P = 0\overset{d}{.}2$ in Table 7. AES must have measured these changes for more than a year, because their $P_{\rm Moon}$ estimate was much closer to $29\overset{d}{.}53$ than the expected observational $\pm 0\overset{d}{.}2$ error.

3.5. Results of the Period Analysis of all S Prognoses

There was no significant periodicity in S prognoses, because all best P failed the criterion of Equation (8). The $P = 30\overset{d}{.}3 \pm 0\overset{d}{.}2$ and $7\overset{d}{.}48 \pm 0\overset{d}{.}02$ for SSTP = 13, 15, ..., 23 were the same within their error limits (Table 8). These P, originating from S at $D = 20$, were replaced by the new $P = 1\overset{d}{.}557$, $2\overset{d}{.}795$, and $2\overset{d}{.}822$ for SSTP = 14, 16, ..., 24. The $2\overset{d}{.}822$ and $2\overset{d}{.}795$ periods were both close, but not equal to, the $2\overset{d}{.}850$ period already detected from G prognoses. $P'(P_0, k_1, k_2) \approx 1\overset{d}{.}55$ was predicted by $P = 2\overset{d}{.}795$, $P_0 = 1\overset{d}{.}0$, $k_1 = 1$, and $k_2 = -1$ (Tanner 1948).

3.6. General Remarks about the Results of Period Analysis

We analyzed 24 different SSTP. We had an infinite number of alternatives for transforming Table 1 into t_i, but we simply could not invent any other realistic alternative transformations that would have altered our period analysis results. For example, the available prognoses for $D = 2$ were always "GGG." We performed additional tests, where t_i at $D = 1$ and 2 were removed. The best period was $2\overset{d}{.}85$. However, we could not test all possible alternatives for removing t_i from the data.

The unreal periods could be divided into two categories. Those of the first category were present even in aperiodic data, like the long periods predicted by Equation (6). Normalization eliminated these first category unreal periods. The second category of unreal periods were induced by the real periods. Some of these unreal periods could be predicted, like the connection between the real $2\overset{d}{.}85$ period and the unreal $1\overset{d}{.}54$ period (Tanner 1948). Normalization did not eliminate these second category unreal periods, but they vanished when the real periodicity was removed, like the unreal $7\overset{d}{.}48$ period when the real $29\overset{d}{.}6$ period was removed. This indicated that only the $29\overset{d}{.}6$ and $2\overset{d}{.}85$ periods were real.

The standard Q estimates were unreliable. For example, the evidence for $P_1 = 2\overset{d}{.}850$ in SSTP = 1 was not indisputable, because it failed the criterion of Equation (5). However, the significance of $P_1 = 2\overset{d}{.}850$ was underestimated ($Q > Q^\star$), while that of $P_2 = 29\overset{d}{.}6$ was overestimated ($Q < Q^\star$). Periods $29\overset{d}{.}6$ and $2\overset{d}{.}850$ reached $z_0 = z_{\rm N}(f) = 16.7$ and 14.6. Inserting these z_0 into Equation (4) gave $Q(z_0) = 0.000013$ and 0.00011. This was nearly equal to $Q^\star = 0.000012$ and 0.00014. We emphasize that Equation (4) should not be applied to $z_{\rm N}(f)$. However, using $z_0 = z_{\rm N}(f)$ in Equation (4) gave $Q(z_0) \approx Q^\star$. This indicated that our simulated statistics were robust.

Normalization allowed us to imitate the pattern of lucky and unlucky days, although we did not know how these were chosen. It gave us the $Q^\star$ estimates and eliminated some of the unreal periods. The best idea of all was to test what happens after removing $P_{\rm Moon}$. This resulted in the $2\overset{d}{.}850$ period being the only significant real period and its significance increased. CC does not give explicit clues as to why AES assigned the prognoses with such regularity, but the $2\overset{d}{.}850$ period differs by $0\overset{d}{.}017 \pm 0\overset{d}{.}002$ from the current orbital period $2\overset{d}{.}867328$ of Algol. If this is indeed the reason for finding this periodicity in CC, then $P_{\rm orb}$ should have increased about $25^{\rm m}$ since 1224 B.C.

Coinciding θ_i of n_1 periodic t_i give $|\mathbf{A_1}| = |\sum_{i=1}^{n_1} \mathbf{r}_i| = n_1$. If aperiodic t_i give $|\mathbf{A_2}| = |\sum_{i=1}^{n-n_1} \mathbf{r}_i| \approx 0$, then $z = |\mathbf{A_1} + \mathbf{A_2}|^2/n \approx n_1^2/n$. For example, $P = 29\overset{d}{.}4$ and $2\overset{d}{.}851$ reached $z = 17.4$ and 12.1 in SSTP = 1 ($n = 564$), which gave $n_1 \geqslant \sqrt{zn} \approx 99$ and 83. If 36 values connected to $P_{\rm Moon}$ were at $D = 1$, the other t_i inducing this signal must have been at $D = 2$, 3, 29, or 30. Thus, most of the G data could be aperiodic, because $n_1 \approx 200$ prognoses could induce $P_{\rm Moon}$ and $P_{\rm Algol}$. The exact required number, n_1, cannot be solved, because the θ_i of all n_1 periodic t_i cannot be equal with Equations (2) and (3). There were 126 eclipses of Algol during $360^{\rm d}$. If AES used *only one* G prognosis to mark each individual eclipse, they may even have marked all eclipses into CC, because reaching $n_1 \gtrsim 83$ requires interpolating many of the ≈60 daytime eclipses or of those eclipses that occurred when Algol was in conjunction with Sun.

We used simulations to check if a signal of n_1 periodic G prognoses with $P_{\rm Algol} = 2\overset{d}{.}85$ would induce the $z(f)$ periodogram of Figure 2(a). We selected these n_1 periodic t_i from the real data of SSTP = 2. We assigned the remaining $n - n_1$ aperiodic random prognoses in such a way that the relative number of different daily prognosis combinations was the same as in the real data (Table 4). Our simulations reproduced the unreal $1\overset{d}{.}54$ period, as well as those predicted by Equation (6). The period of $P_{\rm Algol} = 2\overset{d}{.}85 = 57^{\rm d}/20$ induced a $z(f)$ peak at $P_{\rm Return} = 19^{\rm d}$ in many signals, because a series of eclipses was repeated every 19 days (see Figure 4(a), groups of vertical lines). AES may have noted that eclipses "returned" exactly to the same epoch of the night after $57^{\rm d} = 3 \times 19^{\rm d}$. The relation $P_{\rm Return}/P_{k_3} - P_{\rm Return}/P_{\rm Algol} = k_3 = \pm 1, \pm 2, \ldots$ predicted $z(f)$ peaks at $f = 1/P_{k_3}$. For example, $P_{k_3=1} = 3\overset{d}{.}353$ and $P_{k_3=-1} = 2\overset{d}{.}478$ gave one cycle less or more than $P_{\rm Algol}$ during $P_{\rm Return}$. The $z(f)$ peaks at these unreal P_{k_3} frequently exceeded the $P_{\rm Algol}$ peak in weaker simulated signals ($n_1 = 40$). However, $P_{\rm Algol}$ dominated over P_{k_3} in stronger simulated signals ($n_1 = 100$). When we divided the real STTP = 1 and 2 data into two parts, these unreal P_{k_3} were weaker in the first part of CC ($N_{\rm E} \leqslant 180$), but many P_{k_3} peaks exceeded that of $P_{\rm Algol}$ in the second part ($N_{\rm E} > 180$). The real ($P_{\rm Moon}$ and $P_{\rm Algol}$) and the unreal ($7\overset{d}{.}48$ and $1\overset{d}{.}54$) periods were present in both parts. Our simulations also revealed that the $z(f) = 12.7$ peak at $f = 1/P_{\rm Algol}$ in Figure 2(a) could be reproduced, if AES recorded only the observed, $n_1 \approx 60$, nighttime eclipses by using *more than one* G prognosis for each eclipse. AES may even have attributed importance to a connection between $P_{\rm Moon}$ and $P_{\rm Algol}$, because $P_{\rm Return} = 19^{\rm d}$ coincides with the difference between $D = 1$ (always GGG) and $D = 20$ (always SSS) during *every* month.

The table from the Cosmology of Seti I and Ramses IV given in Neugebauer & Parker (1960, pp. 84–86) demonstrates how prone written documents from ancient Egypt were to writing errors. If we consider the amount of wrongly copied entries in the aforementioned table, it seems fair to test for an estimated 10% of incorrect entries. Therefore, we simulated periodic signals with $n_1 = 60$, where six randomly chosen time points of each simulated signal were displaced. These simulations revealed

that if AES recorded only the observed ≈60 yearly nighttime eclipses in CC, the period of Algol could be discovered although 10% of their entries were erroneous.

Here, we discuss our precision estimate, $\sigma_P = 0\overset{d}{.}002$, for $P_{\rm Algol}$. The maximum separation between three t_i *within* one day is $8^{\rm h} \equiv \Delta\phi = 0.12$ for $P_{\rm Algol}$. An eclipse positioned to a correct third of the day, had $\sigma_{\Delta\phi_i} \approx 0.06$ for Equation (3) and less for Equation (2). Our large samples contained four t_i within each $P_{\rm Algol}$. We obtained our σ_P estimates for $P_{\rm Moon}$ and $P_{\rm Algol}$ from 1 yr of data. The long-term mean of the variable length of synodic month, $P_{\rm syn} = 29\overset{d}{.}53$, was closer to our $P_{\rm Moon}$ than what could be measured from only 1 yr of observations (Section 3.4, last paragraph). This indicated that AES measured $P_{\rm Moon}$ changes over many years. It was easier to measure long-term $P_{\rm Algol}$ than $P_{\rm Moon}$, because the former remained practically constant. A period change of $0\overset{d}{.}017$ would revise the predictions radically, because the current $P_{\rm orb} = 2\overset{d}{.}867$ predicts eclipses about $52^{\rm h}$ later in the end of a year than $P_{\rm orb} = 2\overset{d}{.}850$. The precision of $\sigma_P = 0\overset{d}{.}002$ predicts correct nights for all yearly eclipses, because the accumulated error is only $\pm 6^{\rm h}$.

The ratio $P_{\rm Moon}/P_{\rm Algol} = 29\overset{d}{.}6/2\overset{d}{.}850 = 10.4$ was close to $P_{\rm week} = 10^{\rm d}$. However, five facts contradicted the idea that $P_{\rm week}$ and $P_{\rm Moon}$ induced $P_{\rm Algol}$. (1) There were no signs $P_{\rm week}$ in CC. (2) $P_{\rm Algol} = 2\overset{d}{.}850 \pm 0\overset{d}{.}002$ was $55 \times \sigma_P$ smaller than $P_{\rm Moon}/10 = 2\overset{d}{.}960$. (3) After removing the $D = 1$ prognoses, $P_{\rm Moon}$ and the unreal $7\overset{d}{.}48$ period vanished, but $P_{\rm Algol}$ *did not* vanish (compare Figures 1(c) and 2(c)). Hence, $7\overset{d}{.}48$ was connected to $P_{\rm Moon}$, but $P_{\rm Algol}$ was not. (4) After removing the $D = 1$ prognoses, $P_{\rm Moon}$ vanished, but the significance of $P_{\rm Algol}$ *always* increased (Table 7). This indicated that $P_{\rm Algol}$ was not connected to $P_{\rm Moon}$. (5) The ratio $P_{\rm Moon}/P_{\rm Algol}$ induces a 0.4 phase difference in one month. Events connected to $P_{\rm Moon}$ and $P_{\rm Algol}$ are totally out of phase throughout the whole year. Thus, $P_{\rm Moon}$ and/or $P_{\rm week}$ certainly did not induce $P_{\rm Algol}$.

It could be argued that our test against H_0 was irrelevant, because the data contained an algorithm. The $z(f')$ peaks are at f' that maximize $|\mathbf{R}|$. The values of $|\mathbf{R}|$ or f' do not depend on H_0, but reveal any arbitrary $P' = 1/f'$ coded with an algorithm, e.g., $P_{\rm Moon}$ or $P_{\rm Algol}$. The $z_0 = z(f')$ value would give the Q estimate for P' (Equation (4)), but we emphasized repeatedly that these standard Q estimates were not valid. We identified the best periods P' from the $z_{\rm N}(f')$ peaks, which did not depend on H_0. We solved the critical levels, $Q^\star$, from simulations, which did not rely on H_0. In short, our period analysis results did not depend on H_0.

We also tested the constant daytime, $l_{\rm D}(N_{\rm G}) = 12^{\rm h}$, alternative for all $N_{\rm G}$ of the year (Equations (2) and (3)). The results did not change. The $l_{\rm D}(N_{\rm G})$ changes, and $\delta_\odot(N_{\rm G})$ approximation in Section 2 had no influence on the results.

4. ASTROPHYSICS

The physical parameters of Algol are given in Table 9, where the subscripts "1" and "2" denote the "A–B" and "AB–C" systems. The zero-age main sequence masses were $m_{\rm B} = 2.81\ M_\odot$ and $m_{\rm A} = 2.50\ M_\odot$ in the "best-fitting" evolutionary model of Sarna (1993), where Algol B evolved away from the main sequence in 450 million years. This happened only a few million years ago. Roche-lobe overflow caused substantial MT to Algol A, which became more massive than Algol B within less than 700,000 yr. MT is weaker at the current quiescent stage. The complex APC of Algol may have "masked" (Biermann & Hall 1973) the presence of a small long-term $P_{\rm orb}$ increase that

Table 9
Physical Parameters of the Algol System (Zavala et al. 2010)

Orbital Elements A–B System	Orbital Elements AB–C System	Masses
$a_1 = 2.3 \pm 0.1$	$a_2 = 93.8 \pm 0.2$	$m_{\rm A} = 3.7 \pm 0.2$
$i_1 = 98.6$	$i_2 = 83.7 \pm 0.1$	$m_{\rm B} = 0.8 \pm 0.1$
$\Omega_1 = 7.4 \pm 5.2$	$\Omega_2 = 132.7 \pm 0.1$	$m_{\rm C} = 1.5 \pm 0.1$
$e_1 = 0$	$e_2 = 0.225 \pm 0.005$	
$P_1 = 2.867328$	$P_2 = 679.85 \pm 0.04$	

Note. $[a_1] = [a_2] = {}''/1000$, $[i_1] = [i_2] = [\Omega_1] = [\Omega_2] = {}^\circ$, $[e_1] = [e_2] =$ dimensionless, $[P_1] = [P_2] =$ days, $[m_{\rm A}] = [m_{\rm B}] = [m_{\rm C}] = M_\odot$.

should have been observed as parabolic $O - C$ changes. MT from the less massive Algol B to the more massive Algol A should lead to a long-term increase

$$\dot{P}_{\rm orb}/P_{\rm orb} = -[3\dot{m}_{\rm B}(m_{\rm A} - m_{\rm B})]/(m_{\rm A}m_{\rm B}), \quad (9)$$

where $\dot{P}_{\rm orb}$ is the rate of $P_{\rm orb}$ change, $m_{\rm A}$ and $m_{\rm B}$ are the masses of the gainer and the loser, and $\dot{m}_{\rm B}$ is the MT rate (Kwee 1958, Equation (5)). If $P_{\rm orb}$ was $2\overset{d}{.}850$ in 1224 B.C. and it has since then increased to $2\overset{d}{.}867328$, constant $\dot{P}_{\rm orb}$ would give $\dot{m}_{\rm B} = -2.2 \times 10^{-7}\ M_\odot\ {\rm yr}^{-1}$. This agreed with the "best-fitting" evolutionary model that predicted $\dot{m}_{\rm B} = -2.9 \times 10^{-7}\ M_\odot\ {\rm yr}^{-1}$ (Sarna 1993). Soderhjelm (1980) noted that Algol's MT "is unlikely to be less than $10^{-7}\ M_\odot\ {\rm yr}^{-1}$." Constant MT is only an approximation, because short MT bursts interrupt the long quiescent periods (e.g., Mallama 1978). Equation (9) may also underestimate MT (Zavala et al. 2002). However, more conservative MT estimates, between 10^{-13} and $10^{-8}\ M_\odot\ {\rm yr}^{-1}$, have been published (Harnden et al. 1977; Cugier & Chen 1977; Hadrava 1984; Richards 1992).

Bastian (2000) discussed the accumulated long-term effects of Earth's non-uniform rotation to the $O - C$ diagrams of EB. Such effects also shift the computed epochs of ancient solar eclipses (Smith 2012). However, accumulated effects are insignificant within 1 yr of data, like CC. The days in 1224 B.C. were $0\overset{s}{.}055$ shorter than now, because the increase has been about $0\overset{s}{.}0017$ in a century (Stephenson 1997). If $P_{\rm orb}$ was $2\overset{d}{.}850\,000$ in days in 1224 B.C., it would be $2\overset{d}{.}849\,998$ in modern days. This $0\overset{d}{.}000\,002$ difference was 1000 times smaller than our error $\sigma_P = 0\overset{d}{.}002$ for $2\overset{d}{.}850$ and 8500 times smaller than the $0\overset{d}{.}017$ period change. Hence, Earth's non-uniform rotation did not prevent a reliable comparison of the present-day $P_{\rm orb}$ of Algol to that in 1224 B.C.

The perturbations of Algol C are slowly changing i_1 and eclipses may not always occur. Soderhjelm (1975) derived the period for these i_1 changes

$$P_{i_1} = \frac{4[1+(m_{\rm A}+m_{\rm B})/m_{\rm C}]\left(P_2^2/P_1\right)\left(1-e_2^2\right)^{3/2}}{3[(G_1/G_2)^2 + 2(G_1/G_2)\cos\Psi + 1]^{1/2}\cos\Psi}, \quad (10)$$

where $G_1 = m_1[Ga_1(1-e_1)^2(m_{\rm A}+m_{\rm B})]^{1/2}$, $m_1 = (m_{\rm A}m_{\rm B})/(m_{\rm A}+m_{\rm B})$, $G_2 = m_2[Ga_2(1-e_2)^2(m_{\rm A}+m_{\rm B}+m_{\rm C})]^{1/2}$, $m_2 = [(m_{\rm A}+m_{\rm B})m_{\rm C}]/(m_{\rm A}+m_{\rm B}+m_{\rm C})$, G is the gravitational constant and Ψ is the angle between the orbital planes of A–B and AB–C systems, which fulfills

$$\cos\Psi = \cos i_1 \cos i_2 + \sin i_1 \sin i_2 \cos(\Omega_1 - \Omega_2). \quad (11)$$

Combining $\Psi = 95^\circ \pm 3^\circ$ (Csizmadia et al. 2009) and $\Psi = 86^\circ \pm 5^\circ$ (Zavala et al. 2010) to the values in Table 9 gave

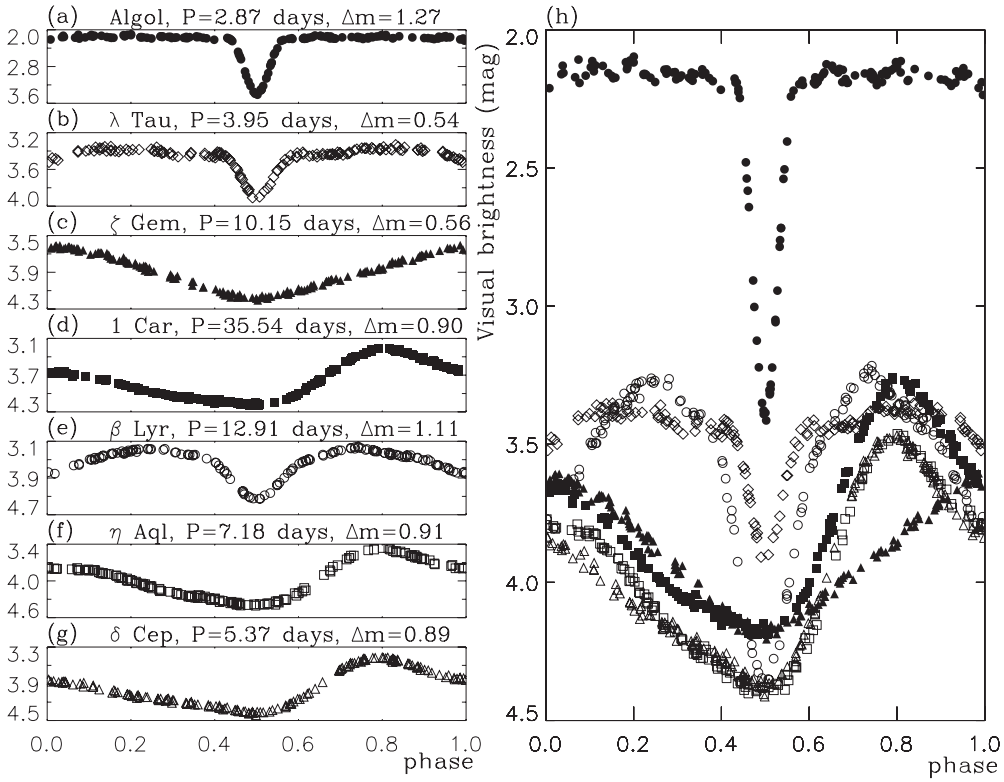

Figure 3. Light curves of the best candidates as function of phase. (a) Algol (closed circles), (b) λ Tau (open diamonds), (c) ζ Gem (closed triangles), (d) l Car (closed squares), (e) β Lyr (open circles), (f) η Aql (open squares), and (g) δ Cep (open triangles). (h) All curves in the same scale: Algol is more than one magnitude brighter than the other six variables and has the largest amplitude.

P_{i_1} = 25,000 and 31,000 yr, i.e., i_1 may have been stable during the past three millennia. The P_{i_1} lower limits were 14,000 and 16,000 yr for $\pm 1\sigma_\Phi$. Therefore, we could not confirm that eclipses occurred in 1224 B.C.

5. ASTRONOMY

Naked eye observers can discover periodicity in the Sun, the planets, the Moon, and the stars. Periods of the Sun and the planets exceed 90^d. $P_{\rm Moon}$ was in CC. Thus, the stars were the only other celestial objects, where AES could have detected periodicity between $1^d.5$ and 90^d. Here, we present eight criteria indicating that Algol was the most probable star, where AES could have discovered periodic variability. The General Catalogue of Variable Stars (hereafter GCVS[3]) gave the maximum brightness ($m_{\rm max}$), the amplitude (Δm), and the period (P) of all known over 40,000 variables. The criterion

C_1: *variability fulfils* $m_{\rm max} \leqslant 4.0$ *and* $\Delta m \geqslant 0.4$

gave those 109 stars, where variability could be discovered with naked eyes (e.g., Turner 1999). The criterion

C_2: *period is known and fulfils* $1^d.5 \leqslant P \leqslant 90^d$

left us with the 13 stars of Table 10. The criterion

C_3: *variable was not below, or too close to, the horizon*

eliminated ζ Pho, β Dor, and κ Pav. The next criterion

C_4: *variability can be predicted*

eliminated ρ Per (Percy et al. 1993, 1996), μ Lep (Renson et al. 1976; Heck et al. 1987; Perry et al. 1987) and R Lyr (Percy et al. 1996, 2001). Their changes cannot be predicted even today. The changes of the remaining candidates are shown in Figures 3 and 4. The light curves have not changed significantly since the discovery of these variables. Therefore, we first modeled the light curves of the photometry in Kim (1989; Algol), Grant (1959; λ Tau), Moffett & Barnes (1980; ζ Gem, η Aql, and δ Cep), Dean et al. (1977; 1 Car), and Aslan et al. (1987; β Lyr). We then obtained a full phase coverage by selecting a random sample of points from these models and adding a Gaussian random $0^m.01$ error to them. This is what anyone would observe with an instrument having a precision of $0^m.01$. These curves could be descriptive, because we were only interested in what can be detected with naked eyes. Algol is easiest to

Table 10
Thirteen Variable Star Candidates Not Rejected with C_1 or C_2

Name	P (days)	Type	$m_{\rm max}$ (mag)	Δm (mag)	δ (deg)	a_0 (hr)	a_{30} (hr)	a_{60} (hr)	$a_{\rm max}$ (deg)
ζ Pho	1.6697671	EB	3.91	0.51	−73	0	0	0	<0
ρ Per	50	SP	3.30	0.70	+23	14	10	6	86
Algol	2.8673043	EB	2.12	1.27	+25	14	10	6	88
λ Tau	3.9529478	EB	3.37	0.54	−1	12	8	4	62
μ Lep	2	CP	2.97	0.44	−25	10	5	0	38
β Dor	9.8426	CE	3.46	0.62	−65	0	0	0	<0
ζ)Gem	10.15073	CE	3.62	0.56	+18	13	9	6	82
l Car	35.53584	CE	3.28	0.90	−50	7	0	0	14
β Lyr	12.913834	EB	3.25	1.11	+34	15	10	6	82
R Lyr	46	SP	3.88	1.12	+43	16	11	7	73
κ Pav	9.09423	CE	3.91	0.87	−60	4	0	0	3
η Aql	7.176641	CE	3.48	0.91	−1	12	8	4	62
δ Cep	5.366341	CE	3.48	0.89	+44	16	11	7	73

Notes. Column 1: name; Column 2: P; Column 3: type (EB: eclipsing binary; SP: semiregular pulsating star; CP: chemically peculiar; or CE: cepheid); Columns 4 and 5: $m_{\rm max}$ and Δm; Column 6: δ in 1224 B.C.; Columns 7–10: time above altitudes 0°, 30°, and 60° (a_0, a_{30}, and a_{60}) and upper culmination ($a_{\rm max}$).

[3] GCVS at http://www.sai.msu.su/groups/cluster/gcvs/gcvs/ was accessed in 2008 November.

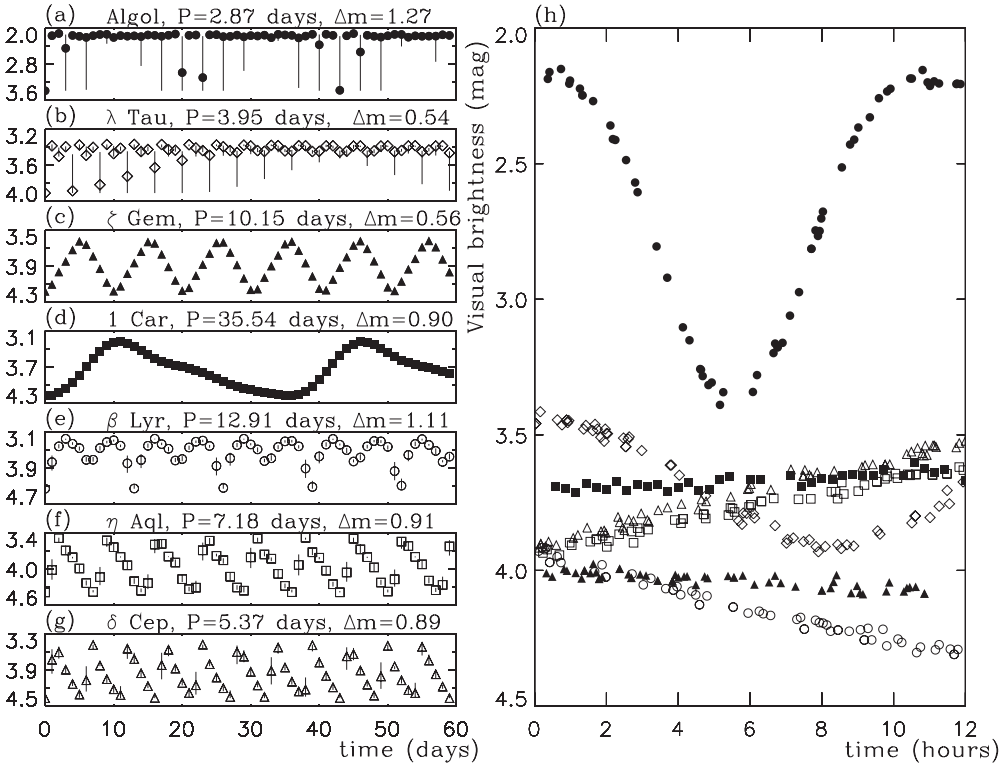

Figure 4. Light curves of the best candidates as a function of time. (a)–(g) The symbols are the same as Figure 3, but here they denote the brightness at mid-night. The vertical lines (when visible) display the total range of the brightness changes during a night lasting 12 hr. (h) The nightly changes in the same scale. The selected phase interval of each light curve is the one that would induce the largest possible changes during a single night.

observe with naked eyes. The next three criteria require that the naked eye observer can *identify* suitable and *eliminate* unsuitable comparison stars. The criterion

C_5: *variability can be detected during a single night*

eliminated ζ Gem and l Car. The largest nightly changes of β Lyr, η Aql, and δ Cep were between $0\overset{m}{.}2$ and $0\overset{m}{.}4$. The vertical lines in Figure 4 show that the changes of these three could not be perceived during most nights. The nightly changes of Algol and λ Tau, $1\overset{m}{.}27$ and $0\overset{m}{.}54$, are the largest. Algol is the only EB, whose entire eclipse can be observed during a single night (Figure 4(h)).

We also checked how easy it is to discover the changes of these seven variables in relation to nearby stars ("⚹" in Figure 5 and Table 11). Our notations for brighter stars, belonging and not belonging to the same modern constellation as "⚹", are large "⋆," and large "•," respectively (Hoffleit & Jaschek 1991; Bright Star Catalogue, hereafter BSC). The notations for comparison stars are small "⋆" and small "•." Table 11 gives the name, BSC number, and m of stars close to "∗." We give Δm, if it exceeds $0\overset{m}{.}05$. The distance from "⚹" is $[d] = {}^\circ$. We compared four aspects: (1) how many large "⋆" and large "•" outshined "⚹"? (2) How many suitable and unsuitable small "⋆" and small "•" were available? (3) What kind of observations were required (Table 10: P, Δm)? (4) What were the extinction effects (Table 10: a_0, a_{30}, a_{60})? The criterion

C_6: *variability changes the constellation pattern*

eliminated all other candidates, except Algol and λ Tau. It favored Algol, the second brightest star in a field, where it fades below all six comparison stars in 5^h (Figure 5(a)).

Our previous criteria lead only to the discovery of *variability*, but not to the discovery of *periodicity*. Discovery of periodicity in the smooth light curves of ζ Gem, l Car, η Aql, δ Cep, and β Lyr requires the tabulation of differential magnitudes (i.e., a *time series*). Even if such tabulation had succeeded, it is unlikely that AES could have used a graphical solution to discover periodicity, like Figures 4(c)–(g). Algol and λ Tau appear constant, except during eclipses. However, no *time series* is required to discover their periodicity, but only a *series of time points.* If the eclipse epochs are found to be multiples of the same number, then periodicity has been discovered. The criterion

C_7: *period of variability could be discovered by AES*

did not eliminate Algol or λ Tau. The former is brighter with a larger Δm, its exact eclipse epochs are easier to determine and its altitude was higher in 1224 B.C.

The history of astronomy should indicate objectively the probability for discovering variability and periodicity. In 1596, Fabricius discovered the first variable, Mira. The next one, Algol, was discovered by Montanari in 1669. Goodricke (1783) discovered its period. Baxendell (1848) discovered the variability and $P_{\rm orb}$ of λ Tau, but it took another 60 yr to measure the light curve due to the lack of suitable comparison stars (Stebbins 1920). The last criterion

C_8: *variability and periodicity was discovered first*

clearly favored Algol. Our eight criteria strongly indicated that Algol was the most probable star, where AES could have discovered periodic variability.

How could we constrain Algol's evolution, if AES, Goodricke, and modern astronomers used different magnitude systems? The time when the light fades, t_i, is the same in any system. Hence, any P inferred from these t_i does not depend on the system.

6. DISCUSSION

AES were socially valued professionals, e.g., in astronomy, mathematics, and medicine. Their duties included also the

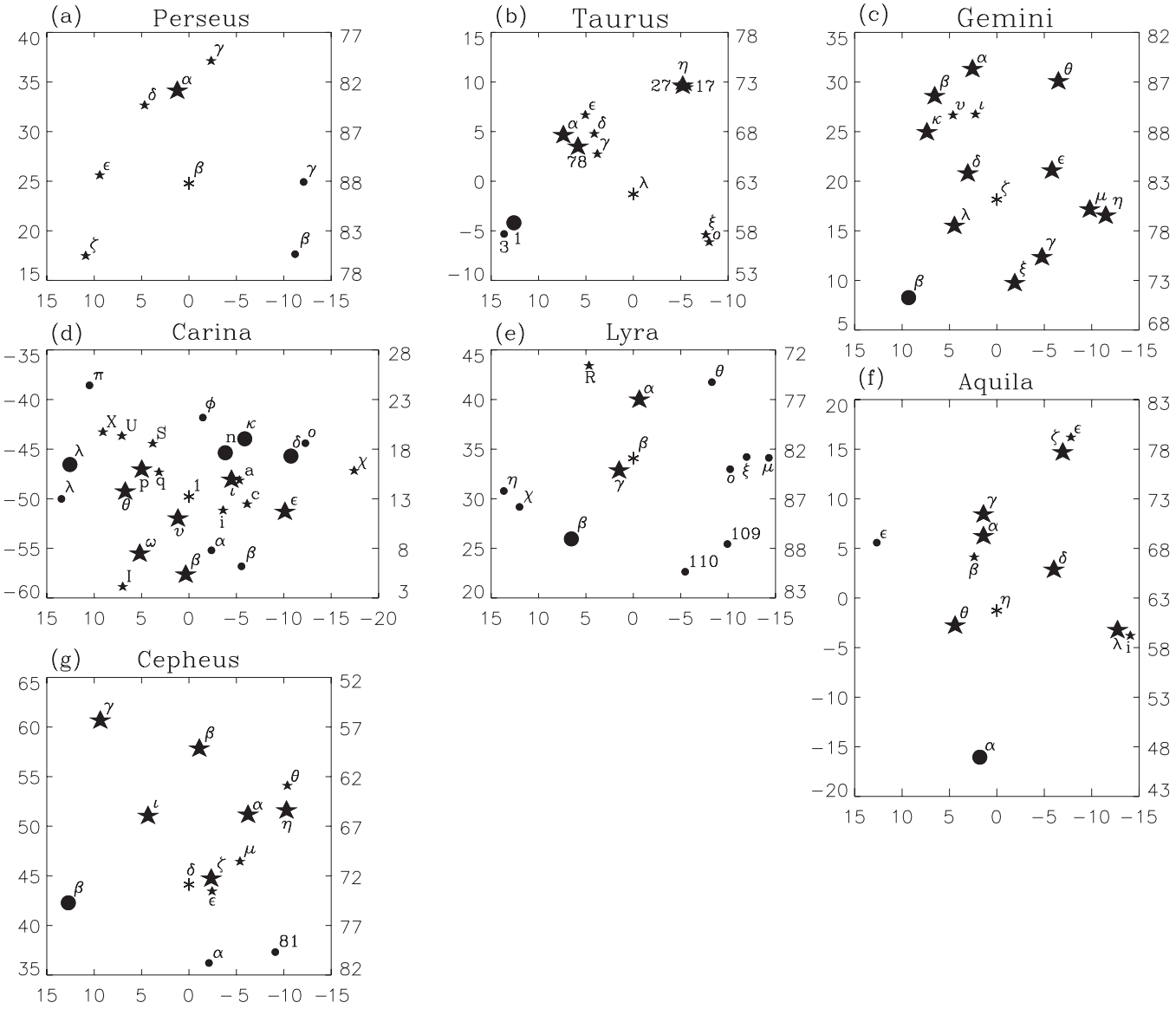

Figure 5. Stars close to the seven best candidates ("⁕"). The stars in the same modern constellation (large and small "⋆") are shown if $d \leqslant 20^\circ$ in Table 11. The stars not belonging to the same modern constellation (large and small "•") are shown if $d \leqslant 15^\circ$. The right ascension (x-axis: (°)), declination (left-hand y-axis: (°)), and the altitude of upper culmination $a_{\max}$ (right-hand y-axis:(°)) have been calculated for 1224 B.C.

measurement of time by observing stars while they conducted the proper nightly rituals that kept the Sun safe during its journey across the underworld (Leitz 1989, 1994; Hardy 2002; Krauss 2002, 2012). The timing of these rituals was important, because it had to appease the terrible guardians, who opened one gate of the underworld at each hour (Clagett 1989). The Sun was reborn at the 12th hour, but only if AES performed the rituals absolutely right. The risk that the Sun would never rise again was imminent. With $P_{\rm Algol} = 57^{\rm d}/20$, the eclipses always occur exactly at the same modern hour after 57 nights. Ancient Egyptian hours were of relative length so in winter the day hours were shorter than in summer, and for night hours the reverse. Also due to the methods they employed to take into account the dawn and the dusk, their measurement of time was not precise (Clagett 1995). If an eclipse was observed in the end of the night, the next eclipses occurred at three night intervals, but always about three and a half hours earlier, until they could not be observed at daytime. This sequence of nighttime eclipses was repeated every 19 days. The eclipses also returned to the same part of the night after 57 days. These regularities occur with modern or ancient hours, or to be precise, they could be discovered without any concept of hours. Whatever Algol "did" (blinked or not) on $D \approx 1$ (always GGG), it always also did on $D \approx 20$ (always SSS). There are nearly 300 clear nights a year in this area (Mikhail & Haubold 1995). Evidence of star clocks, which AES used to measure time from stars, spans over a millennium from the First Intermediate Period (ca. 2181–2055 B.C.) to the Late Period (664–332 B.C.). For this purpose, they devised star tables to help with time keeping (Clagett 1995). For example, the Ramesside star clocks contained 13 rows of stars, where the first row stood for the opening of the night, the next 11 rows for the beginning of the consecutive hours of the night, and the last row stood for the ending of the night. AES must have encountered difficulties in the correct identification of a very bright star (Algol), because it was frequently outshined by six other dimmer nearby stars. This star sometimes even lost and regained its brightness during the same night (midnight eclipse). Either they arrived at a known period value or they just recorded the observed eclipses. AES

Table 11
Brightest Stars Close to the Seven Best Variable Star Candidates

Notation	Name		m (mag)	Δm (mag)	d (°)
large ⋆	α Per	HR 1017	1.79	–	9.4
∗	β Per	HR 936	2.12	1.27	
small ⋆	ζ Per	HR 1203	2.85	–	12.9
small ⋆	ϵ Per	HR 1220	2.88	0.12	9.5
small ⋆	γ Per	HR 915	2.93	–	12.6
small ⋆	δ Per	HR 1122	3.01	–	9.2
small •	γ And	HR 603	2.26	–	12.1
small •	β Tri	HR 622	3.00	–	13.1
large ⋆	α Tau	HR 1457	0.75	0.20	9.4
large ⋆	β Tau	HR 1791	1.65	–	25.7
large ⋆	η Tau	HR 1165	2.87	–	12.1
large ⋆	ζ Tau	HR 1910	2.88	0.29	24.7
large ⋆	78 Tau	HR 1412	3.35	0.07	7.5
∗	λ Tau	HR 1239	3.37	0.54	
small ⋆	ϵ Tau	HR 1409	3.53	–	9.4
small ⋆	o Tau	HR 1030	3.60	–	9.4
small ⋆	27 Tau	HR 1178	3.63	–	11.9
small ⋆	γ Tau	HR 1346	3.65	–	5.5
small ⋆	17 Tau	HR 1142	3.70	–	12.2
small ⋆	ξ Tau	HR 1038	3.70	0.09	8.7
small ⋆	δ Tau	HR 1373	3.76	–	7.3
large •	1 Ori	HR 1543	3.19	–	12.9
small •	3 Ori	HR 1552	3.69	–	14.2
large ⋆	β Gem	HR 2990	1.14	–	12.4
large ⋆	α Gem	HR 2891	1.59	–	13.4
large ⋆	γ Gem	HR 2421	1.93	–	7.5
large ⋆	μ Gem	HR 2286	2.75	0.27	9.8
large ⋆	ϵ Gem	HR 2473	2.98	–	6.5
large ⋆	η Gem	HR 2216	3.15	0.75	11.6
large ⋆	ξ Gem	HR 2484	3.36	–	8.7
large ⋆	δ Gem	HR 2777	3.53	–	4.0
large ⋆	κ Gem	HR 2985	3.57	–	10.1
large ⋆	λ Gem	HR 2763	3.58	–	5.2
large ⋆	θ Gem	HR 2540	3.60	–	13.7
∗	ζ Gem	HR 2650	3.62	0.56	
small ⋆	ι Gem	HR 2821	3.79	–	8.9
small ⋆	υ Gem	HR 2905	4.06	–	9.7
large •	β CMi	HR 2845	2.84	0.08	13.5
large ⋆	α Car	HR 2326	-0.72	–	27.8
large ⋆	β Car	HR 3685	1.68	–	7.9
large ⋆	ϵ Car	HR 3307	1.86	–	10.4
large ⋆	ι Car	HR 3699	2.25	–	4.7
large ⋆	θ Car	HR 4199	2.76	–	6.7
large ⋆	υ Car	HR 3890	3.01	–	2.6
large ⋆	ω Car	HR 4037	3.32	–	8.0
large ⋆	p Car	HR 4140	3.27	0.10	5.5
small ⋆	q Car	HR 4050	3.36	0.08	3.9
small ⋆	a Car	HR 3659	3.44	–	5.5
small ⋆	χ Car	HR 3117	3.47	–	17.1
∗	l Car	HR 3884	3.28	0.90	
small ⋆	U Car	HR 4257	3.78	–	9.0
small ⋆	S Car	HR 4114	3.82	–	6.4
small ⋆	c Car	HR 3571	3.84	–	6.2
small ⋆	X Car	HR 4337	3.84	0.18	10.7
small ⋆	i Car	HR 3663	3.97	–	3.9
small ⋆	I Car	HR 4102	4.00	–	12.0
large •	δ Vel	HR 3485	1.96	0.40	11.1
large •	κ Vel	HR 3734	2.50	–	8.1
large •	n Vel	HR 3803	3.13	–	5.7
small •	ϕ Vel	HR 3940	3.54	–	8.1
small •	o Vel	HR 3447	3.55	0.12	12.8
large •	λ Cen	HR 4467	3.13	–	12.6
small •	π Cen	HR 4390	3.89	–	14.7
small •	β Vol	HR 3347	3.77	–	9.3
small •	α Vol	HR 3615	4.00	–	6.0
small •	λ Mus	HR 4520	3.64	–	13.4
large ⋆	α Lyr	HR 7001	-0.02	0.09	5.9
large ⋆	γ Lyr	HR 7178	3.24	–	2.0
∗	β Lyr	HR 7106	3.25	1.11	
small ⋆	R Lyr	HR 7157	3.88	1.12	10.6
small •	μ Her	HR 6623	3.42	–	14.3
small •	ξ Her	HR 6703	3.70	–	12.0
small •	o Her	HR 6779	3.80	0.07	10.2
small •	109 Her	HR 6895	3.84	–	12.9
small •	θ Her	HR 6695	3.86	–	11.6
small •	110 Her	HR 7061	4.19	–	12.6
large •	β Cyg	HR 7417	3.08	–	10.3
small •	η Cyg	HR 7615	3.39	–	13.8
small •	χ Cyg	HR 7564	3.30	10.9	12.7
large ⋆	α Aql	HR 7557	0.77	–	7.6
large ⋆	γ Aql	HR 7525	2.72	–	9.7
large ⋆	ζ Aql	HR 7235	2.99	–	17.4
large ⋆	θ Aql	HR 7710	3.23	–	4.7
large ⋆	δ Aql	HR 7377	3.36	–	7.2
large ⋆	λ Aql	HR 7236	3.44	–	12.9
small ⋆	β Aql	HR 7602	3.71	–	5.9
∗	η Aql	HR 7570	3.48	0.91	
small ⋆	ϵ Aql	HR 7176	4.02	–	19.2
small ⋆	i Aql	HR 7193	4.02	–	14.3
large •	α Cap	HR 7754	0.08	–	15.0
small •	ϵ Del	HR 7852	4.03	–	14.4
large ⋆	α Cep	HR 8162	2.44	–	9.6
large ⋆	γ Cep	HR 8974	3.21	–	20.0
large ⋆	β Cep	HR 8238	3.16	0.11	13.7
large ⋆	ζ Cep	HR 8465	3.35	–	2.4
large ⋆	η Cep	HR 7957	3.43	–	13.3
large ⋆	ι Cep	HR 8694	3.52	–	8.3
∗	δ Cep	HR 8571	3.48	0.89	
small ⋆	μ Cep	HR 8316	3.43	1.67	5.9
small ⋆	ϵ Cep	HR 8494	4.15	0.06	2.5
small ⋆	θ Cep	HR 7850	4.22	–	15.2
large •	β Cas	HR 21	2.25	0.06	12.7
small •	α Lac	HR 8585	3.77	–	8.2
small •	81 Cyg	HR 8335	4.23	–	11.0

may have considered this variability to threaten the "cosmic order." CC describes the repetitive transformation of the Eye of Horus, usually called "Wedjat" or "the Raging one," from a peaceful to raging personality, with good or bad influence on the life of men (Leitz 1994). A legend existed in which the enraged Eye of Horus nearly destroyed all mankind (Lichtheim 1976). Most likely, AES linked Algol's strange behavior with this prominent legend. It should be noted that in different contexts the concept of the Eye of Horus could embody rather diverse meanings ranging from ritual equipment to even representing "Re," i.e., the Sun (god) (Leitz 2002). It has also been argued that the Eye of Horus represents the Moon (e.g., Sethe 1962; Leitz 1994; Lull & Belmonte 2009), and we discovered $P_{\rm Moon}$ in CC. However, the described repetitive changes of the Eye of Horus seem to follow a much shorter timescale of a few days (Paper III, Section 2).

If AES recorded eclipses, why are there no texts of Algol from other ancient cultures? We argued that AES did not refer directly

to Algol for religious reasons, but used indirect mythological references. Half a year after our manuscript was submitted, Smith (2012) showed that AES also referred to solar eclipses only indirectly. For example, in the passage concerning III Peret 16, according to Leitz' calculations a New Moon day, one is forbidden to go outside and see the darkness (Leitz 1994). The menacing presence of the god Seth over the morning of II Peret 14 has been believed to be a reference to the planet Mercury observed as a morning star (Krauss 2002). Even the most direct astronomical descriptions from the ancient Egyptians such as the Cosmology of Seti I and Ramses IV do not plainly describe what happens in the sky but do that through mythological narrative (Clagett 1995). This could explain the lack of references to the star itself. There are indirect mythological references to Algol also in other ancient cultures (Paper III, Section 8).

The idea that CC contains significant new astrophysical information may appear controversial. A hypothesis is scientific only if it can be tested (e.g., Hempel 1952). Scientific hypotheses are useful if they give predictions based on reasoning, like statistical tests or astrophysical relations. The word "predict" is used here when extrapolating from the present day to 1224 B.C. We use the present day astrophysical parameters of Algol (TEST I: $P_{\rm orb}$, TEST II: $\dot{m}_{\rm B}$, TEST III: Φ) and the present day astronomical catalogs (TEST IV: GCVS, BSC).

Two scientific hypotheses were tested. We rejected our *statistical* hypothesis, H_0, because the $29\overset{\rm d}{.}6$ and $2\overset{\rm d}{.}850$ periods were indisputably detected with the new normalized Rayleigh test. This result was the core of our manuscript.

We applied four tests to our *astrophysical* hypothesis

H_1: *"Period* $2\overset{\rm d}{.}850$ *in CC was* $P_{\rm orb}$ *of Algol."*

TEST I. The present day value is $P_{\rm orb} = 2\overset{\rm d}{.}867$. No one has presented evidence for $P_{\rm orb}$ increase since Goodricke (1783) discovered this period. An astrophysical relation (Equation (9)) predicted that MT from the less massive Algol B to the more massive Algol A should have caused such an increase (Kwee 1958). TEST I supported H_1.

TEST II. The present day MT estimates ($[\dot{m}_{\rm B}] = M_\odot\,{\rm yr}^{-1}$) predicted the following $P_{\rm orb}$ values in 1224 B.C.

Harnden et al. (1977): $|\dot{m}_{\rm B}| \geqslant 10^{-9} \Rightarrow P_{\rm orb} \leqslant 2\overset{\rm d}{.}867$.
Cugier & Chen (1977): $|\dot{m}_{\rm B}| \approx 10^{-13} \Rightarrow P_{\rm orb} \leqslant 2\overset{\rm d}{.}867$.
Soderhjelm (1980): $|\dot{m}_{\rm B}| > 10^{-7} \Rightarrow P_{\rm orb} < 2\overset{\rm d}{.}860$.
Hadrava (1984): $|\dot{m}_{\rm B}| \approx 10^{-8} \Rightarrow P_{\rm orb} \approx 2\overset{\rm d}{.}866$.
Richards (1992): $10^{-11} \leqslant |\dot{m}_{\rm B}| \leqslant 10^{-10} \Rightarrow P_{\rm orb} \leqslant 2\overset{\rm d}{.}867$.
Sarna (1993): $|\dot{m}_{\rm B}| \approx 2.87 \times 10^{-7} \Rightarrow P_{\rm orb} \approx 2\overset{\rm d}{.}845$.

This large range, $10^{-13} \leqslant |\dot{m}_{\rm B}| \leqslant 2.87 \times 10^{-7}$, gave no unique $P_{\rm orb}$ prediction. However, these $|\dot{m}_{\rm B}|$ were based on different approaches: observations and models. The long quiescent periods are sporadically interrupted by short bursts of MT. All conservative MT estimates were based on observations (Harnden et al. 1977; Cugier & Chen 1977; Richards 1992), which may have coincided with the long quiescent periods. The bursts cause $P_{\rm orb}$ changes of several seconds in a year (e.g., Frieboes-Conde et al. 1970; Mallama 1978). MT in these bursts has to be much larger than our estimate, $|\dot{m}_{\rm B}| = 2.2 \times 10^{-7}$, which predicts $P_{\rm orb}$ changes of only $0\overset{\rm s}{.}43$ in a year. Our $|\dot{m}_{\rm B}|$ estimate, based on H_1, may turn out to be valuable, because many MT bursts must have occurred since 1224 B.C. TEST II did not contradict H_1.

TEST III. A naked eye observer can determine $P_{\rm orb}$ from the present day eclipses. Eclipses have not necessarily occurred in all periods of history, because Algol C changes i_1. One argument against H_1 would have been that the present day Ψ (Csizmadia et al. 2009; Zavala et al. 2010) did not prove that eclipses occurred in 1224 B.C. The astrophysical relations of Equations (10) and (11) predicted this. A few days *after* we submitted our manuscript, Baron et al. (2012) published a revised value, $\Psi = 90\overset{\circ}{.}2 \pm 0\overset{\circ}{.}32$, which proved that eclipses similar to the present-day eclipses occurred also in 1224 B.C. We could even argue that H_1 predicted their result. TEST III did not contradict H_1.

TEST IV. We searched for *all* celestial objects, where periodicity between $1\overset{\rm d}{.}5$ and $90^{\rm d}$ could be discovered with naked eyes. $P_{\rm Moon}$ was in this range, but the periods of the Sun and the planets were not. We applied eight criteria to the present day data (GCVS, BSC) to eliminate all unsuitable variable stars. The two most suitable remaining celestial objects were certainly the Moon and Algol. We detected periodic signs of *only* these two celestial objects in CC. TEST IV supported H_1.

TESTS I and IVsupported H_1. TESTS II and III did not contradict H_1, but indicated that H_1 could be true. Thus, we could not prove that H_1 is definitely true. Then again, no one from any field of science has argued what *other* terrestrial or celestial phenomenon occurred regularly every third day, but *always* 3 hr and 36 minutes earlier than before, and caught the attention of AES.

7. CONCLUSIONS

We discovered connections between Algol and AES writings that can hardly be a coincidence. All statistical, astrophysical, astronomical, and egyptological details matched. The period recorded in CC may represent a valuable constraint for future studies of MT in EBs. Goodricke's achievement in 1783 was outstanding. The same achievement by AES, if true, was literally fabulous.

We thank M.A. Patricia Berg, Dr. Robert J. Demaree, PhD Heidi Jauhiainen, Professor Karri Muinonen, and Professor Heikki Oja for reviewing the original manuscript. We thank Nadia Drake, Charles Choi, Anne Liljeström, and Stephen Battersby for encouragement received. The SIMBAD database at CDS and NASA's Astrophysics Data System (ADS) were used. This work was supported by the Vilho, Yrjö and Kalle Väisälä Foundation (P.K.), the Finnish Graduate School in Astronomy and Space Physics (J.Le.), and the Academy of Finland (J.T.-V.).

REFERENCES

Applegate, J. H. 1992, ApJ, 385, 621
Aslan, Z., Derman, E., Engin, S., & Yilmaz, N. 1987, A&AS, 71, 597
Bakir, A. 1966, The Cairo Calendar No. 86637 (Cairo, Egypt: Government Printing Office)
Baron, F., Monnier, J. D., Pedretti, E., et al. 2012, ApJ, 752, 20
Bastian, U. 2000, IBVS, 4822, 1
Batchelet, E. 1981, Circular data in Biology (London: Academic)
Baxendell, J. 1848, MNRAS, 9, 37
Biermann, P., & Hall, D. S. 1973, A&A, 27, 249
Clagett, M. 1989, Ancient Egyptian Science 1: Knowledge and Order (Philadelphia, PA: American Philosophical Society)
Clagett, M. 1995, Ancient Egyptian Science 2: Calendars, Clocks and Astronomy (Philadelphia, PA: American Philosophical Society)
Csizmadia, S., Borkovits, T., Paragi, Z., et al. 2009, ApJ, 705, 436
Cugier, H., & Chen, K.-Y. 1977, Ap&SS, 52, 169
Dean, J. F., Cousins, A. W. J., Bywater, R. A., & Warren, P. R. 1977, MmRAS, 83, 69
Demaree, R., & Janssen, J. 1982, Gleanings from Deir el-Medina (Leiden, Netherlands: Nederlands Instituut voor het Nabije Oosten te Leiden)
Frieboes-Conde, H., Herczeg, T., & Høg, E. 1970, A&A, 4, 78
Goodricke, J. 1783, RSPTA, 73, 474
Gradshteyn, I. S., & Ryzhik, I. M. 1994, Table of Integrals, Series and Products (London: Academic)

Grant, G. 1959, ApJ, 129, 78
Hadrava, P. 1984, BAICz, 35, 335
Hall, D. S. 1989, SSRv, 50, 219
Hardy, P. A. 2002, Arch, 17, 48
Harnden, F. R., Jr., Fabricant, D., Topka, K., et al. 1977, ApJ, 214, 418
Heck, A., Mathys, G., & Manfroid, J. 1987, A&AS, 70, 33
Helck, W., Otto, E., & Westendorf, W. 1975–1992, Läxikon der Ägyptologie, I–VI (Wiesbaden, Germany: Harrassowitz)
Hempel, C. G. 1952, Fundamentals of Concept Formation in Empirical Science (Chicago, IL: Univ. Chicago Press)
Hoffleit, D., & Jaschek, C. 1991, The Bright Star Catalogue (5th ed.; New Haven, CT: Yale Univ. Observatory)
Jetsu, L. 1996, A&A, 314, 153
Jetsu, L. 1997, A&A, 321, L33
Jetsu, L., Hackman, T., Hall, D. S., et al. 2000, A&A, 362, 223
Jetsu, L., & Pelt, J. 1996, A&AS, 118, 587
Jetsu, L., & Pelt, J. 2000, A&A, 353, 409
Jetsu, L., Pelt, J., & Tuominen, I. 1999, A&A, 351, 212
Jetsu, L., Pohjolainen, S., Pelt, J., & Tuominen, I. 1997, A&A, 318, 293
Kim, H. 1989, ApJ, 342, 1061
Kiseleva, L. G., Eggleton, P. P., & Mikkola, S. 1998, MNRAS, 300, 292
Krauss, R. 2002, Alter Orient und Altes Testament, 297, 193
Krauss, R. 2012, Palarch's J. Archaeol. Egypt/Egyptol., 9, 1
Kwee, K. K. 1958, BAN, 14, 131
Lanza, A. F. 2006, MNRAS, 369, 1773
Lehtinen, J., Jetsu, L., Hackman, T., Kajatkari, P., & Henry, G. W. 2011, A&A, 527, A136
Lehtinen, J., Jetsu, L., Hackman, T., Kajatkari, P., & Henry, G. W. 2012, A&A, 542, A38
Leitz, C. 1989, Studien zur Ägyptischen Astronomie (Ägyptologische Abhandlungen 49; Wiesbaden, Germany: Harrassowitz Verlag)
Leitz, C. 1994, Tagewählerei (Ägyptologische Abhandlungen 55; Wiesbaden, Germany: Harrassowitz Verlag)
Leitz, C. 2002, Lexikon der ägyptischen Götter und Götterbezeichnungen Band I (Orientalia Lovaniensia Analecta 432–433; Leuven, Belgium: Peeters)
Liao, W.-P., & Qian, S.-B. 2010, MNRAS, 405, 1930
Lichtheim, M. 1976, Ancient Egyptian Literature II: The New Kingdom (Los Angeles, CA: Univ. California Press)
Lull, J., & Belmonte, J. A. 2009, The Constellations of Ancient Egypt (Cairo, Egypt: Supreme Council of Antiquities Press)
Lyytinen, J., Jetsu, L., Kajatkari, P., & Porceddu, S. 2009, A&A, 499, 601
Lyytinen, J., Johansson, P., Jetsu, L., et al. 2002, A&A, 383, 197
Mallama, A. D. 1978, PASP, 90, 706
Mikhail, J. S., & Haubold, H. J. 1995, Ap&SS, 228, D7
Moffett, T. J., & Barnes, T. G., III. 1980, ApJS, 44, 427
Neugebauer, O., & Parker, R. 1960, Egyptian Astronomical Texts I (London: Brown Univ. Press)
Percy, J. R., Desjardins, A., Yu, L., & Landis, H. J. 1996, PASP, 108, 139
Percy, J. R., Ralli, J. A., & Sen, L. V. 1993, PASP, 105, 287
Percy, J. R., Wilson, J. B., & Henry, G. W. 2001, PASP, 113, 983
Perry, C. L., Olsen, E. H., & Crawford, D. L. 1987, PASP, 99, 1184
Porceddu, S., Jetsu, L., Markkanen, T., & Toivari-Viitala, J. 2008, Camb. Archaeol. J., 18, 327
Renson, P., Manfroid, J., & Heck, A. 1976, A&AS, 23, 413
Richards, M. T. 1992, ApJ, 387, 329
Sarna, M. J. 1993, MNRAS, 262, 534
Scargle, J. D. 1982, ApJ, 263, 835
Sethe, K. 1962, Übersetzung und Kommentar zu den altägyptischen Pyramidentexten V (Hamburg, Germany: Verlag J.J. Augustin)
Smith, D. G. 2012, Egyptol. J., Artic., 6
Soderhjelm, S. 1975, A&A, 42, 229
Soderhjelm, S. 1980, A&A, 89, 100
Stebbins, J. 1920, ApJ, 51, 193
Stephenson, F. R. 1997, Historical Eclipses and Earth's Rotation (Cambridge: Cambridge Univ. Press)
Stephenson, F. R., & Baolin, L. 1991, Obs, 111, 21
Tanner, R. W. 1948, JRASC, 42, 177
Turner, D. G. 1999, JRASC, 93, 228
Zavala, R. T., Hummel, C. A., Boboltz, D. A., et al. 2010, ApJL, 715, L44
Zavala, R. T., McNamara, B. J., Harrison, T. E., et al. 2002, AJ, 123, 450